haematologica
Journal of the Ferrata Storti Foundation

Characterization of JNJ-80948543 a novel CD79bxCD20xCD3 trispecific antibody for B-cell non-Hodgkin lymphoma

by Anna Kuchnio, Danlin Yang, Nele Vloemans, Ivo Cornelissen, Ricardo Amorim, Tatiana Perova, Cassandra Lowenstein, Lut Janssen, Toon Suls, Mariette Bekkers, Elena Lasorsa, Lorena Fontan, Neeharika Nemani, Taylor Hojnacki, Chao Han, Siddharth Sukumaran, Nicole Medeiros, Srimathi Srinivasan, Bingyuan Wu, Jun Chen, Michael D. Feldkamp, Sam Wu, Habtom Habte, Autumn J. McRee, Nikki Daskalakis, John Krayer, Cam Holland, Ricardo Attar, M. Phillip DeYoung, Sanjaya Singh, Yusri Elsayed and Ulrike Philippar

Received: June 25, 2025.
Accepted: February 13, 2026.

Citation: Anna Kuchnio, Danlin Yang, Nele Vloemans, Ivo Cornelissen, Ricardo Amorim, Tatiana Perova, Cassandra Lowenstein, Lut Janssen, Toon Suls, Mariette Bekkers, Elena Lasorsa, Lorena Fontan, Neeharika Nemani, Taylor Hojnacki, Chao Han, Siddharth Sukumaran, Nicole Medeiros, Srimathi Srinivasan, Bingyuan Wu, Jun Chen, Michael D. Feldkamp, Sam Wu, Habtom Habte, Autumn J. McRee, Nikki Daskalakis, John Krayer, Cam Holland, Ricardo Attar, M. Phillip DeYoung, Sanjaya Singh, Yusri Elsayed and Ulrike Philippar. Characterization of JNJ-80948543 a novel CD79bxCD20xCD3 trispecific antibody for B-cell non-Hodgkin lymphoma.
Haematologica. 2026 Feb 26. doi: 10.3324/haematol.2025.288473 [Epub ahead of print]

Characterization of JNJ-80948543 a novel CD79bxCD20xCD3 trispecific antibody for B-cell non-Hodgkin lymphoma

Anna Kuchnio,[1] Danlin Yang,[2°] Nele Vloemans,[1] Ivo Cornelissen,[1] Ricardo Amorim,[1] Tatiana Perova,[3] Cassandra Lowenstein,[2°] Lut Janssen,[1] Toon Suls,[1] Mariette Bekkers,[1] Elena Lasorsa,[1] Lorena Fontan,[1] Neeharika Nemani,[3] Taylor Hojnacki,[3] Chao Han,[4°] Siddharth Sukumaran,[4] Nicole Medeiros,[2] Srimathi Srinivasan,[3°] Bingyuan Wu,[2] Jun Chen,[2] Michael D. Feldkamp,[2] Sam Wu,[2] Habtom Habte,[2] Autumn J McRee,[3] Nikki Daskalakis,[3] John Krayer,[4] Cam Holland,[4] Ricardo Attar,[3] M. Phillip DeYoung,[3] Sanjaya Singh,[2°] Yusri Elsayed,[3] Ulrike Philippar[1]

[1]Oncology, Johnson & Johnson, Beerse, Belgium; [2]Therapeutics Discovery Product Development and Supply, Johnson & Johnson, Spring House, PA, USA; [3]Oncology, Johnson & Johnson, Spring House, PA, USA; [4]Preclinical Sciences & Translational Safety, Johnson & Johnson, Spring House, PA, USA

[°]DY: Currently at Third Arc Bio Inc., Boston, MA, USA

[°]CL: Currently at Third Arc Bio Inc., Philadelphia, PA, USA

[°]CH: Currently at Tavotek Biotherapeutics, Lower Gwynedd, PA, USA

[°]SS: Currently at Merck, Boston, MA, USA

Corresponding author:

Ulrike Philippar
Oncology, Johnson & Johnson,
Turnhoutseweg 30, 2340 Beerse, Belgium
Phone: +32 14603965
E-mail: uphilipp@its.jnj.com

Authorship contributions
AK, DY, NV, IC, RA, TP, LJ, TS, MB, NN, TH, EL, LF, CS, NM, BW, JC, MF, CH, SW, HH, UP performed research. AK, DY, TP, EL, LF, SriSri, SidSuk, AM, ND, JK, CH, RA, MPD, YE, UP discussed and analyzed data. AK and UP wrote the manuscript, which was edited and approved by all authors.

Conflict of Interest Disclosures
All the co-authors are current or in the past 2 years have been employees of Johnson & Johnson and may own stock/stock options in Johnson & Johnson.

Data sharing statement: The data supporting the findings of this study are available within the article or its supplementary materials.

Acknowledgements
This study was funded by Johnson & Johnson. Medical writing support was provided by Paul Cao (Johnson & Johnson) and was funded by Johnson & Johnson.

ABSTRACT (215/250 words)

Despite advances in targeted therapies, relapsed/refractory B-cell non-Hodgkin lymphoma (R/R B-NHL) remains incurable in the majority of patients. Thus, there is a critical need to expand the treatment options for R/R B-NHL to improve patient outcomes. In this study, we characterized JNJ-80948543, a novel trispecific T-cell engager (TCE), designed to target $CD79b^+$ and/or $CD20^+$ lymphoma cells and bind to CD3 T cells with low affinity. By engaging two tumor-antigens, JNJ-80948543 may enhance tumor binding through avidity effects, potentially improving eradication of heterogeneous cell populations and reducing the risk of antigen escape. Preclinical data confirmed potent T-cell–mediated cytotoxicity against $CD79b^+$ and/or $CD20^+$ cells, with increased potency upon dual antigen engagement, consistent with an avidity effect. To mitigate cytokine release syndrome and T-cell exhaustion commonly associated with TCEs, JNJ-80948543 was designed with a low-affinity CD3 arm. In vitro, JNJ-80948543 achieved effective cytotoxicity with lower cytokine release compared to a matched high-affinity CD3 trispecific, JNJ-80948556. Despite reduced cytokine secretion by JNJ-80948543, both antibodies demonstrated comparable antitumor activity in xenograft mouse model. Collectively, the selectivity, potent cytotoxicity, tumor growth inhibition, and favorable cytokine profile of JNJ-80948543 supports its clinical development. Phase 1 clinical trials are ongoing to evaluate JNJ-80948543 as a monotherapy (NCT05424822) and in combination with a co-stimulatory bispecific antibody (NCT06139406) in patients with R/R B-NHL.

Keywords: Aggressive Non-Hodgkin's Lymphoma; Cell Therapy and Immunotherapy; Molecular Pharmacology

INTRODUCTION

B-cell non-Hodgkin lymphoma (B-NHL) is the most common hematological malignancy worldwide. Cluster of differentiation (CD)20 and CD79b are validated therapeutic targets in multiple B-cell malignancies due to restricted B-cell and B-NHL cell expression. Over the past decades, several CD79b- and CD20-targeting monoclonal antibodies (mAbs), including rituximab (CD20 mAb), and subsequent next-generation CD20-mAbs, polatuzumab vedotin (CD79b-antibody drug conjugate [ADC]), have been developed and are clinically effective when used in combination with chemotherapy for treating different subtypes of B-NHL. However, despite advances in treatment, there remains a high incidence of relapsed and refractory disease. Further efforts are needed to develop more effective targeted therapies for patients with B-cell malignancies whose disease no longer responds to standard chemotherapy or immunotherapies. T-cell engaging (TCE) antibodies recognize CD3 on T cells and specific antigens on malignant cells. Several bispecific TCEs, such as CD20xCD3 and CD19xCD3, have shown promising clinical response rates[1], providing proof of concept that this therapeutic approach can be highly effective in treating B-cell malignancies. Notably, multiple CD20×CD3 bispecific antibodies—epcoritamab, glofitamab, and mosunetuzumab—have received regulatory approval, underscoring their clinical impact. However, their long-term efficacy in advanced cancers remains limited due to resistance mechanisms such as target antigen downregulation/loss or intratumor heterogeneity.[2,3]

CD79b is a critical component of the B-cell receptor (BCR), essential for its functionality, signal initiation, and signal transduction. CD79b mutations have been described as oncogenic drivers in diffuse large B-cell lymphoma (DLBCL), resulting in constitutive activation of the nuclear factor kappa-light-chain-enhancer of activated B cells (NF-κB) pathway.[4] Furthermore, a large proportion of B-NHL, including DLBCL and Burkitt lymphoma, are dependent on CD79b expression for survival, independent of its mutational status.[4-6] In

addition, CD79b surface expression has also been shown to remain detectable upon tumor relapse/progression from previous standard-of-care treatment regimens.[7,8] Taken together, CD79b is an attractive target for a TCE approach, as the development of resistance to CD79b-targeted agents through antigen loss may be less likely to occur.[9]

CD20 is a transmembrane protein involved in B-cell activation and differentiation and is present on all mature B cells and most B-NHL cells.[10] CD20 is organized in the plasma membrane as multimeric molecular complexes with other cell-surface and cytoplasmic proteins involved in BCR-activated calcium entry and contributes to signal transduction and B-cell proliferation.[11] Simultaneous targeting of B-cell lineage targets by combining CD20- and CD79b-targeted therapeutics with different mechanisms of action (ADC combined with antibody dependent cellular cytotoxicity [ADCC], /phagocytosis [ADCP], /complement dependent cytotoxicity [CDC] or TCE) have been explored in the clinical setting (NCT04231877, NCT04594798, NCT03671018, NCT04665765, NCT04479267, NCT04182204) and showed some improved efficacy with a favorable safety profile in patients with relapsed or refractory (R/R) B-cell lymphoma.[12-15] However, no dual CD79b and CD20 targeted TCE approaches have been explored to date.[12-14,16]

Here, we describe a novel trispecific TCE antibody targeting CD79b, CD20, and CD3, JNJ-80948543, to facilitate T-cell mediated cytotoxicity of $CD79b^+$ and/or $CD20^+$ tumor cells both in vitro and in vivo. JNJ-80948543 was designed to induce proximity between T cells and B-cell NHL tumor cells, promoting immunological synapse formation and subsequent tumor cell lysis through perforin and granzyme release by cytotoxic T lymphocytes (CTLs). JNJ-80948543 incorporates a low-affinity CD3 binding arm to mitigate cytokine release syndrome (CRS) and T-cell exhaustion, while JNJ-80948556 features a higher-affinity CD3 arm to enhance T-cell activation. Preclinical studies using cellular models with varying CD79b and CD20 expressions explored the impact of dual antigen engagement on cytolytic

potential. In vivo xenograft models demonstrated potent antitumor activity for both constructs, with JNJ-80948543 showing reduced in vitro cytokine release compared to JNJ-80948556.

METHODS

Generation of CD79bxCD20xCD3 trispecifics

JNJ-80948543 and JNJ-80948556 feature mutations in the fragment crystallizable (Fc) region to abolish interaction with Fc receptors. Heterodimerization was enhanced using the knobs-into-holes platform mutations. JNJ-80948543 contains a low-affinity and JNJ-80948556 a higher-affinity anti-CD3 single-chain variable fragment (scFv) fused onto the N-terminus of the 'knob' Fc region and an anti-CD20 scFv attached to the C-terminus of the Fc region. The 'hole' chain comprises a high-affinity CD79b antigen-binding fragment and contains mutations to disrupt protein A binding of monomeric and homodimerized hole chains.

Cell lines and cell culture

All cell lines used were of human origin and obtained from either American Type Culture Collection or Deutsche Sammlung von Mikroorganismen und Zellkulturen. cell lines were cultured in RPMI 1640 medium with GlutaMAX and with 10% fetal bovine serum without antibiotics at 37°C in a 5% carbon dioxide incubator.

T cell–mediated cytotoxicity and T-cell activation using cell lines and healthy donor T-cells

For the in vitro assays, tumor cell lines were plated with thawed purified frozen T cells at 5:1 or 1:1 effector to target ratio (E:T) and trispecific antibody (TsAb) or control antibodies and incubated at 37°C with 5% carbon dioxide for 48 or 72 hours. The supernatant was collected for cytokine analysis, and the cells were stained for analysis on a FACSLyric or

FACSymphony A1 cell analyzers (BD Biosciences). Cytotoxicity was assessed by quantifying viable carboxyfluorescein succinimidyl ester positive (CFSE□) cancer cells per well. Viable cells in these assays were determined using Fixable Viability Dye eFluor™ 780.

Cytotoxicity (%) was calculated as:

$$\text{Cytotoxicity} = \left(\frac{\text{Absolute \# viable cancer cells}}{\text{Average \# viable cancer cells in untreated wells}}\right) \times 100$$

T-cell activation was measured by CD69 and CD25 expression on CD4□ and/or CD8□ T cells.

Cytokine measurement

Supernatants were collected from in vitro T-cell cytotoxicity assays. Production of interferon-γ, interleukin (IL)-1β, IL-2, IL-4, IL-6, IL-10, IL-12p70, IL-13, and tumor necrosis factor (TNF)-α was assayed by using the Meso Scale Discovery (MSD) human pro-inflammatory panel 1 kit as per the instructions. An additional single-plex analysis from MSD for granulocyte-macrophage colony-stimulating factor (GM-CSF) was also performed according to the manufacturer's protocol.

CD79b antagonistic studies

The effect of JNJ-80948543 on CD79b downstream signaling was assessed by evaluating the inhibition of IL-10 secretion by MSD. The MSD assay was performed as described per manufacturer's protocol.

Xenograft studies

All experiments were carried out in accordance with The Guide for the Care and Use of Laboratory Animals and were approved by the Institutional Animal Care and Use Committee of Johnson & Johnson, Beerse, Belgium.

Further details can be found in the Supplemental Methods section.

RESULTS

Generation and specificity characterization of JNJ-80948543

JNJ□80948543 is a novel TsAb binding to the epsilon subunit of the CD3 T-cell receptor complex (CD3□; Uniprot ID P07766), CD79b (B-cell antigen receptor complex-associated protein β chain; Uniprot ID P40259) and CD20 (B lymphocyte antigen CD20; Uniprot ID P11836) tumor antigens **(Figure 1A)**. JNJ-80948543 features mutations in the Fc region to abolish interaction with Fc receptors.

Each binding arm of JNJ-80948543 was evaluated for binding specificity in the Retrogenix® Cell Microarray Technology screen (Charles River Laboratories) and confirmed to be specific for the respective primary targets (data not shown). JNJ-80948543 was also shown to be specific for CD20 and CD79b in an in vitro functional assay (cytokine release) using a panel of 6 cancer cell lines that lack expression of CD79b and CD20, but in transcriptomics are predicted to express >50% of the known cell surface proteins using a transcript per million cut-off of >5 **(Supplemental Figure 1)**.

Expression of CD79b and CD20 in cancer cell lines and patient samples

The lineage markers, CD79b and CD20, are expressed in early to mature stages of normal B-cell development, and both antigens are undetectable in terminally differentiated plasma

cells. CD79b and CD20 were highly expressed in several subtypes of B-NHL, including DLBCL, follicular lymphoma, and mantle cell lymphoma **(Supplemental Figure 2A-D)**. In the majority of B-NHL samples, CD79b and CD20 were co-expressed, but within each B-NHL type there were up to 25% of cells that expressed either CD79b or CD20 **(Supplemental Figure 2B)**. Using immunohistochemistry, CD79b and CD20 were also detected in formalin-fixed paraffin-embedded tissues obtained from patients with B-NHL at initial diagnosis or from those with R/R disease following treatment with R-CHOP (rituximab–cyclophosphamide–hydroxydaunorubicin–oncovin–prednisone/prednisolone) **(Supplemental Figure 2D)**. Additionally, analysis of receptor density in cell lines confirmed that CD79b and CD20 expression was largely restricted to B-NHL cells and was not observed in malignant cells from other lineages **(Supplemental Table 1)**.

JNJ-80948543 binding profiles to B-NHL cell lines and CD3$^+$ T cells

JNJ-80948543 acts as a bridge between tumor cells and T cells by binding CD79b and CD20 on target tumor cells and CD3 on T cells. To reduce the frequency and/or severity of CRS, T-cell anergy and T-cell exhaustion induced by TCE therapies, JNJ-80948543 was designed with a low-affinity CD3 binding arm (SPR, KD 221 nM). In lymphoma cell lines with varying CD79b and CD20 densities **(Supplemental Table 1)**, JNJ-80948543 demonstrated stable binding to tumor cells over 48 hours **(Figure 1B and 1C)**. Higher concentrations of JNJ-80948543 were needed for binding to human T cells expressing endogenous CD3 compared with B-NHL cell lines, due to the low-affinity CD3 binding arm **(Figure 1D and Supplemental Figure 3A)**.

JNJ-80948543 exhibits increased avidity and cytotoxic potency

JNJ-80948543 facilitates the formation of an immunological synapse by binding to both CD79b and CD20, initiating T-cell activation and enabling cytotoxicity of tumor cells by

secretion of perforin and granzymes stored in the secretory vesicles of CTLs. Expression of both targets on a tumor cell could potentially result in dual antigen-binding by JNJ-80948543, leading to increased avidity and cytotoxic potency. To address this question, TCE assays were performed using K562 target cells engineered to express CD79b, CD20, or both antigens **(Figure 2A)**. JNJ-80948543 induced concentration-dependent cytotoxicity of target cells expressing either CD79b or CD20. The NullxCD20xCD3 antibody only induced concentration-dependent cytotoxicity of the K562_CD20 target cells and not the K562_CD79b cells. The activity of the NullxCD20xCD3 antibody with target cells expressing both antigens (K562_CD79b_CD20) was similar to that observed when incubated with K562_CD20 target cells. In contrast, when the assay was conducted with K562_CD79b_CD20 cells, JNJ-80948543 induced much greater cytotoxicity, which is approximately 1,000-fold greater than the potency observed with target cells expressing either antigen. These results are consistent with an avidity effect.

To further corroborate the benefit of dual tumor antigen targeting, in vitro cytotoxicity of $CD20^+$ $CD79b^+$ B-NHL cell lines (WSU-DLCL2, OCI-Ly10, and CARNAVAL) was assessed in the presence of JNJ-80948543, CD79bxNullxCD3, or NullxCD20xCD3, and T cells from healthy donors as effector cells. CD79bxNullxCD3 or NullxCD20xCD3 both showed cytotoxic activity, however, with lower potency as compared with JNJ-80948543 **(Figure 2B, Supplemental Table 2)**. T-cell activation and proliferation in co-culture of $CD79b^+/CD20^+$ cancer cells were higher in the presence of JNJ-80948543 than CD79bxNullxCD3, or NullxCD20xCD3 control antibodies **(Figure 2C, Supplemental Figure 3B)**. Altogether, the data indicated that JNJ-80948543 may be effective in targeting tumor cells that express CD79b and/or CD20 and confirmed that dual tumor antigen-binding by JNJ-80948543 results in increased avidity and cytotoxic potency.

JNJ-80948543 induces in vitro T-cell activation and T cell-mediated cytotoxicity of tumor cells independent of level of CD79b and CD20

To further characterize the activity of JNJ-80948543, B-NHL cell lines with varying levels of CD20 and CD79b expression **(Supplemental Table 1)** were incubated with purified healthy human T cells in the presence of JNJ-80948543 for 48 or 72 hours. JNJ-80948543 induced T cell–mediated cytotoxicity of all $CD79b^{+}/CD20^{+}$ cell lines **(Figure 3A and Supplemental Table 3)** without eliciting a cytotoxic response to $CD79b^{-}/CD20^{-}$ cell lines K562 and SU-DHL1 **(Figure 3A)**. As expected, the negative control antibodies (NullxNullxCD3) did not exhibit any cytotoxicity.

Recent immunoprofiling studies in DLBCL highlighted substantial differences in T-cell infiltration in cold and hot DLBCL tumors. Hot DLBCL tumors are characterized by high immune infiltration, whereas cold DLBCL tumors exhibit low immune cell presence, indicating an immune-depleted microenvironment.[17,18] To assess the impact of increased target burden on the cytotoxic potential of JNJ-80948543 in vitro, tumor cell viability in the presence of treatment and purified human pan $CD3^{+}$ T cells was also assessed at a 1:1 E:T ratio, that might be more relevant in context of cold DLBCL tumors, after either 48 or 72 hours. JNJ-80948543 induced T-cell mediated cytotoxicity but with lower maximum cytotoxicity and higher EC_{50} values in comparison to a 5:1 E:T ratio **(Figure 3B, Supplemental Table 3)**.

In parallel, T-cell activation, measured by the level of CD25 expression on T cells, was assessed. JNJ-80948543 mediated T-cell activation only when incubated with $CD79b^{+}/CD20^{+}$ cell lines, but not in the presence of the $CD79b^{-}/CD20^{-}$ cell lines, demonstrating the specificity of T-cell activation (**Figure 4A, Supplemental Figure 4A)**. Similarly, a negative

control NullxNullxCD3 antibody did not induce significant T-cell activation in any of the cell lines.

To further characterize T-cell activation induced by JNJ-80948543, supernatants from the in vitro cytotoxicity assay were analyzed for cytokine levels using MSD. JNJ-80948543, engineered with a low-affinity CD3 arm, demonstrated T-cell activation accompanied by low cytokine release across tested cell lines (**Figures 4B**, **Supplemental Figures 4B and 4C**). JNJ-80948556 (**Supplemental Figure 5A**) is a matched CD79bxCD20xCD3 TsAb designed with a higher affinity CD3 (SPR, KD ~10-50 nM) compared to JNJ-80948543's CD3 affinity (SPR, KD 221 nM) and was included for comparison purposes. JNJ-80948556 (CARNAVAL, EC_{50}: 11 nM; OCI-Ly10 EC_{50}: 55 nM) showed comparable cancer cell binding to JNJ-80948543 (CARNAVAL EC_{50}: 8 nM; OCI-Ly10 EC_{50}: 43.4 nM), with stable engagement over 48 hours (**Figure 1B, 1C** and **Supplemental Figure 5C, 5D**). However, unlike JNJ-80948543 (EC_{50} > highest tested concentration 1µM) (**Figure 1D**), JNJ-80948556 demonstrated dose-dependent binding to T cells, with an EC_{50} of 104 nM (**Supplemental Figure 5B**). These findings confirm that the CD3 binding arm is the only distinguishing feature between the two molecules. When comparing cytokine secretion with these two TsAbs at 48 hours in T-cell cytotoxicity assays with OCI-Ly10 and CARNAVAL cells (**Supplemental Figures 5E, 5F**), JNJ-80948543 induced lower cytokine levels than JNJ-80948556. This suggests that JNJ-80948543 can drive effective T-cell–mediated cytotoxicity with low cytokine secretion (**Supplemental Table 4**).

JNJ-80948543 mediates CD79b$^+$CD20$^+$ tumor cell cytotoxicity in human whole blood

To evaluate the impact of JNJ-80948543 in a more physiologically relevant setting, T-cell cytotoxicity assays were conducted using healthy human whole blood as a source of T-cell effectors, and in co-culture with fluorescently labeled CD79b$^+$CD20$^+$ CARNAVAL or OCI-

Ly10 cells. Both non-malignant B cells from the whole blood and added tumor cells were evaluated for cytolysis. T-cell activation and serum cytokine levels were also evaluated. JNJ-80948543 elicited concentration-dependent cytotoxicity of $CD20^+CD79b^+$ CARNAVAL and OCI-Ly10 cells after 48 and 72 hours **(Figure 5A and 5B)** with concomitant T-cell activation **(Figures 5C and 5D)**, but with low cytokine secretion **(Supplemental Figures 6A and Supplemental Figure 6B)**.

JNJ-80948543 also elicited concentration-dependent cytotoxicity of non-malignant autologous B cells in the presence of CARNAVAL and OCI-Ly10 cells after 48 and 72 hours **(Supplemental Figures 6C and 6D)**. At 72 hours, the median EC_{50} of JNJ-80948543-induced T-cell mediated autologous B-cell depletion was 0.459 and 0.563 nM in the presence of CARNAVAL and OCI-Ly10 cells, respectively.

Also, in an autologous assay set up without added cancer cells, JNJ-80948543 induced T-cell mediated non-malignant autologous B-cell depletion **(Figure 5E**), with a median EC_{50} of 1.19 nM. T cells were also activated in a concentration-dependent manner in the presence of JNJ-80948543 after 48 or 72 hours of incubation, as measured by the frequency of $CD25^+$ on $CD8^+$ T cells **(Figure 5F)**. Cytokine release varied across donors. In the tested concentration range, no plateau was reached for the majority of the cytokines and cytokine release was observed mostly at highest tested concentrations of JNJ-80948543, in line with its lower-affinity CD3 binding arm **(Supplemental Figure 6E)**.

CD79b antagonistic activity of JNJ-80948543

Phosphorylation of CD79a and CD79b initiates BCR signaling. One of the prominent downstream signaling pathways engaged after BCR stimulation is the classical NF-κB pathway, which is frequently activated in ABC-DLBCL due to oncogenic mutations in CD79a/b.[4] NF-κB signaling regulates the expression of multiple cytokines, including IL-10.

The ability of JNJ-80948543 to inhibit the secretion of IL-10 was assessed by OCI-Ly10 and HBL-1 ABC DLBCL cells harboring either CD79a ITAM or CD79b mutations. JNJ-80948543 elicited a concentration-dependent inhibition of IL-10 secretion by OCI-Ly10 and HBL-1 cells **(Figure 5G, 5H)**. To provide evidence that this effect on IL-10 secretion was solely dependent on CD79b binding, matched CD79bxNullxCD3, NullxCD20xCD3 and NullxNullxCD3 control antibodies were included along JNJ-80948543. NullxCD20xCD3 and NullxNullxCD3 antibodies did not show any effect on IL-10 inhibition, while CD79bxNullxCD3 and JNJ-80948543 had overlapping activities in both cell lines **(Figure 5G, 5H)**. These results demonstrate that JNJ-80948543 inhibits IL-10 secretion and potentially affects BCR signaling. Further experiments are necessary to comprehensively validate its impact on NF-κB signaling and its broader effects on the BCR pathway.

JNJ-80948543-induced T-cell-mediated tumor growth inhibition of B-cell lymphoma xenografts in vivo

In vivo efficacy of JNJ-80948543 was evaluated in 2 independent DLBCL models: CARNAVAL (prevention tumor model) and OCI-Ly10 (established tumor model). In the CARNAVAL prevention model (**Figure 6A, Supplemental Figure 7A**), twice a week intraperitoneal (IP) treatment with JNJ-80948543 or vehicle (Dulbecco's phosphate-buffered saline [DPBS]) was administered after subcutaneous (SC) injection of tumor cells. At Day 22, 1 or 5 mg/kgJNJ-80948543 prevented tumor growth in the majority of mice, resulting in 95% and 100% tumor growth inhibition (TGI), respectively. In the OCI-Ly10 established model (**Figure 6B, Supplemental Figure 7B**), twice a week treatment starting at Day 14 with 3 or 10 mg/kg JNJ-80948543 or vehicle was administered in mice with tumor volumes averaging 108 mm^3. On Day 34 treatment ended, and complete responses were observed in 8 of 10 and 10 of 10 mice treated with 3 or 10 mg/kg JNJ-80948543 by day 38,

respectively (**Figure 6B**). At Day 38, treatment with 3 or 10 mg/kg JNJ-80948543 resulted in 92% or 98% tumor regression (TR), respectively, as compared with the vehicle. A parallel evaluation of JNJ-80948556 in the established OCI-Ly10 model at identical dose levels (3 or 10 mg/kg) demonstrated in vivo efficacy comparable to JNJ-80948543 (**Supplemental Figure 7C**).

JNJ-80948543 mediates T-cell tumor infiltration

The effects of JNJ-80948543 treatment on T-cell tumor infiltration were assessed in the OCI-Ly10 DLBCL established SC tumor model. After four doses, a trend of TGI was observed in mice treated with 1.0 or 3.0 mg/kg JNJ-80948543 compared with vehicle-treated mice **(Supplemental Figure 7D)**. After the fourth dose was administered, tumor samples were harvested at 4, 24, 72, 96, and 168 hours to assess human $CD8^+$ tumor-infiltrating T cells **(Figure 6C)**. A marked increase of tumor-infiltrating $CD8^+$ T cells was observed with 3.0 mg/kg JNJ-80948543 at 4 hours compared with vehicle-treated tumors. Higher levels of $CD8^+$ T cells were observed at 72 and 168 hours in tumors treated with 3 mg/kg JNJ-80948543. Similar results were observed in tumors treated with 1 mg/kg JNJ-80948543 (data not shown). These results demonstrate that treatment with JNJ-80948543 resulted in tumor infiltration of $CD8^+$ T cells.

While NSG mouse models enable engraftment of human lymphoma cells and assessment of T-cell–mediated cytotoxicity, it does not capture the complexity of immune interactions present in patients. As a result, immune modulation and cytokine dynamics could not be fully evaluated in this setting. Future clinical studies will be essential to confirm these observations and assess the broader immunological effects of JNJ-80948543.

DISCUSSION

In this study, we describe a novel TsAb TCE targeting CD79b, CD20, and CD3, JNJ-80948543, that binds to T cells and $CD79b^+$ and/or $CD20^+$ B-NHL, enabling potent and specific T-cell–mediated cytotoxicity in vitro and in vivo. JNJ-80948543 effectively eliminated tumor cells expressing varying levels of CD79b or CD20 in vitro.

Dual targeting of CD79b and CD20 addresses key limitations of current therapies. While Rituximab-based regimens have improved outcomes in patients with DLBCL, approximately 20–40%[19] will recur and require novel options. Several different treatment modalities have been approved in the last decade or are currently in clinical testing for B-NHL, including monoclonal enhanced effector and bispecific TCE antibodies, ADCs, and chimeric antigen receptor T (CAR-T) cells, primarily target single antigens (CD19, CD20, and CD79b). However, no dual CD79b and CD20 targeted TCE approaches have been explored to date.

Clinical combination studies underscore the potential benefit of dual tumor antigen targeting. Polatuzumab vedotin (CD79b-ADC) in combination with bendamustine and rituximab showed improvement in complete response and progression-free survival (PFS) as compared with bendamustine and rituximab in patients with R/R DLBCL after failure of two or more lines of therapy.[13] These results led to the accelerated approval of Pola-BR by the US Food and Drug Administration in 2019.[12] Additionally, the combination of polatuzumab vedotin and rituximab plus cyclophosphamide, doxorubicin, and prednisone (Pola-R-CHP) showed significant improvement in PFS in previously untreated DLBCL patients compared with R-CHOP[14], leading to the approval of Pola-R-CHP regimen in many countries (2022/2023). Also, phase 1b/2 trial of mosunetuzumab (CD20xCD3 TCE) plus polatuzumab vedotin in R/R aggressive LBCL demonstrated a favorable safety profile with highly durable responses.[16] This concept aligns with emerging strategies in combining CD20×CD3

bispecific antibodies with other agents. For example, epcoritamab plus R-CHOP achieved an objective response rate (ORR) of 100% and CR of 87% in previously untreated LBCL patients (EPOCORE-NHL 2). Similarly, glofitamab combined with polatuzumab vedotin and rituximab (Pola-R-CHP) demonstrated high complete response (CR) rates in high-risk LBCL patients (NCT06047080), and a chemotherapy-light regimen of glofitamab, rituximab, and polatuzumab (R-Pola-Glo) is being evaluated in elderly/unfit patients (NCT05798156). In the R/R setting, mosunetuzumab plus polatuzumab vedotin significantly improved PFS compared to Rituximab, Gemcitabine en Oxaliplatin in the phase III SUNMO trial (NCT05171647). This concept aligns with emerging strategies in cellular therapies, where dual-target CAR-T constructs are in clinical evaluation. CD19/CD20 CAR-T therapies have demonstrated ORR up to 91% and CR rates of 73% in R/R B-NHL with manageable CRS and low immune effector cell-associated neurotoxicity syndrome (ICANS) incidence.[20] Similarly, CD19/CD22 CAR-T approaches report ORR of 83.7% and CR of 78% across multiple trials[21], with a recent Phase II study showing 100% ORR and 67.7% CR in LBCL (NCT06081478). Furthermore, tri-specific CAR-T constructs targeting CD19/CD20/CD22 (NCT07168486) are under investigation to further mitigate antigen escape. These developments highlight the therapeutic rationale for multi-antigen targeting across modalities, reinforcing the potential of JNJ-80948543 to deliver improved efficacy and durability in B-NHL.

Treatment relapse after B-cell lineage targeted therapies have been linked to antigen loss. Profiling B-NHL samples showed that up to 25% of cells expressed either CD79b or CD20. Previous studies reported that loss of CD20 expression, ranging from 7.9–60%, attributed to reduced transcription or acquisition of truncating mutations have been reported as mechanisms for resistance to anti-CD20 therapies including rituximab and mosunetuzumab.[2,22-28] Unlike CD20, antigen loss of CD79b does not appear to be a major driver of resistance in both pre-clinical and clinical studies. For example, CD79b antigen loss

as a mechanism for resistance to polatuzumab vedotin for DLBCL has not been largely observed.[13] Lack of CD79b antigen loss is likely not observed due to its requirement for BCR signal transduction. It was shown that loss of CD79b signaling led to reduced survival of ABC and GCB DLBCL, and Burkitt lymphoma.[4-6] Furthermore, ablation or nonsense mutations of CD79a or CD79b were observed in B-lymphocyte deficient mice and resulted in the developmental arrest of B cells at the pre-B cell stage.[29] Taken together, these studies indicate that CD79b is an attractive target for a TCE approach, as the development of resistance to CD79b-targeted agents through antigen loss may be less likely to occur. Therefore, as characterized in this study, the dual antigen-targeting properties of JNJ-80948543 could potentially prevent occurrences of R/R disease in patients with B-NHL. Dual tumor-antigen targeting with a TCE TsAbs has only recently been exploited[30,31] and has a potential to maximize tumor eradication in the presence of a heterogeneous cell population[32-34] and prevent treatment resistance by tumor antigen escape, resulting in sustained response to treatment.

CRS and ICANS are commonly observed with CAR-T cell therapy and CD3 bispecific TCE antibodies.[35,36] Although CRS can be managed in the clinic with step-up dosing schedules, corticosteroid pre-medications and pharmacological inhibition of IL-6R or TNFa, improving the design of next generation CD3 TCEs to reduce the incidence of high-grade CRS is warranted for improved safety and less frequent hospitalizations. Initial TCEs were often biased towards high-affinity CD3 binders[37], which elicited potent tumor cell cytotoxicity but with a high level of cytokine release that required patients to be treated in the hospital with longer periods of steroids. Direct comparison of JNJ-80948543 and JNJ-80948556 in vitro, revealed that CD79bxCD20xCD3 TsAb with higher affinity CD3 resulted higher cytokine secretion.

JNJ-80948543 was engineered with a low-affinity CD3 binding arm to reduce T-cell mediated toxicity, aiming to improve safety and position the TCE as a preferred combination partner in future lymphoma studies. In this preclinical study, JNJ-80948543 induced cytotoxicity of $CD79b^+$ and/or $CD20^+$ tumor cells with corresponding T-cell activation, while eliciting lower cytokine secretion compared to the higher-affinity TsAb, JNJ-80948556. Despite this difference in cytokine release, both molecules demonstrated comparable efficacy in xenograft model. Based on these findings, JNJ-80948543 was prioritized for clinical evaluation. Moreover, these results support the concept that JNJ-80948543 has the potential to uncouple tumor cell cytotoxicity from excessive cytokine release, potentially offering lymphoma patients a curative therapy with an improved benefit-risk profile. Further comparisons with other clinically relevant immunotherapies would help contextualize its therapeutic potential.

B-cell aplasia (BCA) is a recognized on-target effect of B-cell–directed therapies, with its extent and duration varying by antigen and modality. Agents targeting CD19, which is broadly expressed from early B-cell stages to plasma cells, tend to cause more profound and prolonged B-cell depletion compared to those targeting CD20 or CD79b. CAR-T therapies generally induce more profound and sustained BCA compared to TCEs, reflecting differences in mechanism and persistence. For JNJ-80948543, while in vitro studies indicate an impact on healthy B cells, its clinical effect on BCA still to be evaluated in ongoing trials.

In conclusion, JNJ-80948543 exhibited potent and specific elimination of CD79b and/or CD20-expressing cells with favorable cytokine profile. Phase 1 clinical trials are ongoing to evaluate JNJ-80948543 as a monotherapy (NCT05424822) and as combination therapy (NCT06139406) with a costimulatory molecule in patients with R/R B-NHL.

References

1. Abou Dalle I, Dulery R, Moukalled N, et al. Bi- and Tri-specific antibodies in non-Hodgkin lymphoma: current data and perspectives. Blood Cancer J. 2024;14(1):23.
2. Schuster SJ, Huw LY, Bolen CR, et al. Loss of CD20 expression as a mechanism of resistance to mosunetuzumab in relapsed/refractory B-cell lymphomas. Blood. 2024;143(9):822-832.
3. Philipp N, Kazerani M, Nicholls A, et al. T-cell exhaustion induced by continuous bispecific molecule exposure is ameliorated by treatment-free intervals. Blood. 2022;140(10):1104-1118.
4. Davis RE, Ngo VN, Lenz G, et al. Chronic active B-cell-receptor signalling in diffuse large B-cell lymphoma. Nature. 2010;463(7277):88-92.
5. He X, Klasener K, Iype JM, et al. Continuous signaling of CD79b and CD19 is required for the fitness of Burkitt lymphoma B cells. EMBO J. 2018;37(11):e97980.
6. Phelan JD, Young RM, Webster DE, et al. A multiprotein supercomplex controlling oncogenic signalling in lymphoma. Nature. 2018;560(7718):387-391.
7. Dornan D, Bennett F, Chen Y, et al. Therapeutic potential of an anti-CD79b antibody–drug conjugate, anti–CD79b-vc-MMAE, for the treatment of non-Hodgkin lymphoma. Blood. 2009;114(13):2721-2729.
8. Fornecker L-M, Muller L, Bertrand F, et al. Multi-omics dataset to decipher the complexity of drug resistance in diffuse large B-cell lymphoma. Sci Rep. 2019;9(1):895.
9. Ormhoj M, Scarfo I, Cabral ML, et al. Chimeric Antigen Receptor T Cells Targeting CD79b Show Efficacy in Lymphoma with or without Cotargeting CD19. Clin Cancer Res. 2019;25(23):7046-7057.
10. Prevodnik VK, Lavrenčak J, Horvat M, Novakovič BJ. The predictive significance of CD20 expression in B-cell lymphomas. Diagn Pathol. 2011:6:33.
11. Bubien JK, Zhou L-J, Bell PD, Frizzell RA, Tedder TF. Transfection of the CD20 cell surface molecule into ectopic cell types generates a Ca2+ conductance found constitutively in B lymphocytes. J Cell Biol. 1993;121(5):1121-1132.
12. Davis JA, Shockley A, Herbst A, Hendrickson L. Polatuzumab Vedotin for the Front-Line Treatment of Diffuse Large B-Cell Lymphoma: A New Standard of Care? J Adv Pract Oncol. 2023;14(1):67-72.
13. Sehn LH, Herrera AF, Flowers CR, et al. Polatuzumab Vedotin in Relapsed or Refractory Diffuse Large B-Cell Lymphoma. J Clin Oncol. 2020;38(2):155-165.
14. Tilly H, Morschhauser F, Sehn LH, et al. Polatuzumab Vedotin in Previously Untreated Diffuse Large B-Cell Lymphoma. N Engl J Med. 2022;386(4):351-363.
15. Amaya ML, Jimeno A, Kamdar M. Polatuzumab vedotin to treat relapsed or refractory diffuse large B-cell lymphoma, in combination with bendamustine plus rituximab. Drugs Today (Barc). 2020;56(4):287-294.
16. Budde LE, Olszewski AJ, Assouline S, et al. Mosunetuzumab with polatuzumab vedotin in relapsed or refractory aggressive large B cell lymphoma: a phase 1b/2 trial. Nat Med. 2024;30(1):229-239.
17. Tumuluru S, Godfrey JK, Cooper A, et al. Integrative genomic analysis of DLBCL identifies immune environments associated with bispecific antibody response. Blood. 2025;145(21):2460-2472.
18. Dai Y, Kizhakeyil A, Chihara D, et al. Multi-modal spatial characterization of tumor immune microenvironments identifies targetable inflammatory niches in diffuse large B□cell lymphoma. Nat Genet. 2025;57(11):2715-2727.
19. Pennings ER, Durmaz M, Visser O, et al. Treatment and outcomes for patients with relapsed or refractory diffuse large B-cell lymphoma: a contemporary, nationwide, population-based study in the Netherlands. Blood Cancer J. 2024;14(1):3.
20. Yang J, Guo H, Han L, Song Y, Zhou K. Dual-targeted CAR T-cell immunotherapies for hematological malignancies: latest updates from the 2023 ASH annual meeting. Exp Hematol Oncol. 2024;13(1):25.

21. Yuan X, Wang F, Zhao P, et al. Efficacy and safety of CD19 combined with CD22 or CD20 chimeric antigen receptor T-cell therapy for hematological malignancies. Front Immunol. 2025;16:1577360.
22. Ang Z, Paruzzo L, Hayer KE, et al. Alternative splicing of its 5'-UTR limits CD20 mRNA translation and enables resistance to CD20-directed immunotherapies. Blood. 2023;142(20):1724-1739.
23. Johnson NA, Leach S, Woolcock B, et al. CD20 mutations involving the rituximab epitope are rare in diffuse large B-cell lymphomas and are not a significant cause of R-CHOP failure. Haematologica. 2009;94(3):423-427.
24. Rushton CK, Arthur SE, Alcaide M, et al. Genetic and evolutionary patterns of treatment resistance in relapsed B-cell lymphoma. Blood Adv. 2020;4(13):2886-2898.
25. Kennedy GA, Tey SK, Cobcroft R, et al. Incidence and nature of CD20-negative relapses following rituximab therapy in aggressive B-cell non-Hodgkin's lymphoma: a retrospective review. Br J Haematol. 2002;119(2):412-416.
26. Hiraga J, Tomita A, Sugimoto T, et al. Down-regulation of CD20 expression in B-cell lymphoma cells after treatment with rituximab-containing combination chemotherapies: its prevalence and clinical significance. Blood. 2009;113(20):4885-4893.
27. Marshalek JP, Qing X, Dragan M, Tomassetti S. Retrospective Study of CD20 Expression Loss in Relapsed or Refractory B-Cell Non-Hodgkin Lymphoma. J Hematol. 2024;13(6):268-277
28. Vinti L, Pianese J, Carraro E, et al. CD20-Negative Relapsed/Refractory Mature B-Cell Non-Hodgkin Lymphomas and Mature B-Cell Leukemia in Children, Adolescent and Young Adults: A Retrospective Review. Blood. 2024;144:3086.
29. Shulzhenko N, Morgun A, Matzinger P. Spontaneous mutation in the Cd79b gene leads to a block in B-lymphocyte development at the C' (early pre-B) stage. Genes Immun. 2009;10(8):722-726.
30. Pillarisetti K, Yang D, Luistro L, et al. Ramantamig (JNJ-79635322), a novel T-cell-engaging trispecific antibody targeting BCMA, GPRC5D, and CD3, in multiple myeloma models. Blood. 2025 Oct 16. doi: 10.1182/blood.2025030027 [Epub ahead of print]
31. Zhang J, Zhou Z. Preclinical study of a novel tri-specific anti-CD3/CD19/CD20 T cell-engaging antobody as a potentially better treatment for NHL. Blood. 2020;136(Supplement 1):22.
32. Ysebaert L, Quillet-Mary A, Tosolini M, Pont F, Laurent C, Fournié J-J. Lymphoma heterogeneity unraveled by single-cell transcriptomics. Front Immunol. 2021;12:597651.
33. Yang Y, Wang Y, Jin X, He W. Single-cell RNA-sequencing reveals cellular heterogeneity and immune microenvironment characteristics between ocular adnexal mucosa-associated lymphoid lymphoma and IgG4− related ophthalmic disease. Front Immunol. 2025;16:1508559.
34. Ye X, Wang L, Nie M, et al. A single-cell atlas of diffuse large B cell lymphoma. Cell Rep. 2022;39(3):110713.
35. Teachey DT, Rheingold SR, Maude SL, et al. Cytokine release syndrome after blinatumomab treatment related to abnormal macrophage activation and ameliorated with cytokine-directed therapy. Blood. 2013;121(26):5154-5157.
36. Moore PA, Zhang W, Rainey GJ, et al. Application of dual affinity retargeting molecules to achieve optimal redirected T-cell killing of B-cell lymphoma. Blood. 2011;117(17):4542-4551.
37. Wu Z, Cheung N. T cell engaging bispecific antibody (T-BsAb): from technology to therapeutics. Pharmacol Ther. 2018;182:161-175.

Figure legends

Figure 1. JNJ-80948543 profiling for binding to cancer cells and T cells.

(A) JNJ-80948543 trispecific antibody schematic.

(B) Dose-dependent binding of JNJ-80948543 to CARNAVAL and OCI-Ly10 B-NHL cells at 1 hour. Data from single experiment with 3 independent replicates are graphed as mean ± SEM.

(C) Binding of JNJ-80948543 over time (up to 48 hours) to CARNAVAL and OCI-Ly10 B-NHL cells. Data from two independent experiments are graphed as mean ± SEM (n=2 replicates).

(D) Binding of JNJ-80948543 to primary T-cell from 3 donors after 1 hour 37°C incubation. Experiment was performed once with 3 T cell donors. Data are graphed as mean ± SEM.

B-NHL, B-cell non-Hodgkin lymphoma; SEM, standard error of the mean.

Figure 2. JNJ-80948543 mediates cytotoxicity of CD79b$^+$ and CD20$^+$ tumor cells and its activity is increased when binding to both tumor antigens.

(A) Effect of JNJ-80948543 and NullxCD20xCD3 antibodies on cytotoxicity of K562 tumor cells expressing CD79b and/or CD20 in the presence of T cells from healthy donors at 5:1 E:T ratio. T cells from 2 healthy donors were incubated with the indicated antibodies, and cell lines expressing CD79b and/or CD20. The percent cytotoxicity over a 6-day assay is graphed as average means ± SEM.

(B) Effect of JNJ-80948543, CD79bxNullxCD3 and NullxCD20xCD3 antibodies on cytotoxicity of WSU-DLCL2, OCI-Ly10, CARNAVAL tumor cells expressing CD79b and

CD20 in the presence of T cells from healthy donors at 5:1 E:T ratio for 72 hours. Data are graphed as mean ± SEM (n=3 independent T-cell donors). Significance in activity between JNJ-80948543 and Null control antibodies was calculated using Two-way ANOVA and the Bonferroni multiple comparison test: WSU-DLCL2 cells JNJ-80948543 vs CD79bxNullxCD3 ($p= 0.0023$), JNJ-80948543 vs NullxCD20xCD3 ($p< 0.0001$), JNJ-80948543 vs NullxNullxCD3 ($p< 0.0001$); OCI-Ly10 cells JNJ-80948543 vs CD79bxNullxCD3 ($p<0.0001$), JNJ-80948543 vs NullxCD20xCD3 ($p<0.0001$), JNJ-80948543 vs NullxNullxCD3 ($p=0.0001$); CARNAVAL cells JNJ-80948543 vs CD79bxNullxCD3 ($p=0.0002$), JNJ-80948543 vs NullxCD20xCD3 ($p=0.0007$), JNJ-80948543 vs NullxNullxCD3 ($p<0.0001$).

(C) Effect of JNJ-80948543, CD79bxNullxCD3 and NullxCD20xCD3 antibodies on T-cell activation in cytotoxicity assays conducted in the presence of WSU-DLCL2, OCI-Ly10, CARNAVAL tumor cells and T cells from healthy donors at 5:1 E:T ratio for 72 hours.

Data are graphed as mean ± SEM (n=3 independent T-cell donors). Significance in activity between JNJ-80948543 and Null control antibodies was calculated using Two-way ANOVA and the Bonferroni multiple comparison test: WSU-DLCL2 cells JNJ-80948543 vs CD79bxNullxCD3 ($p<0.0001$), JNJ-80948543 vs NullxCD20xCD3 ($p<0.0001$), JNJ-80948543 vs NullxNullxCD3 ($p<0.0001$); OCI-Ly10 cells JNJ-80948543 vs CD79bxNullxCD3 ($p<0.0001$), JNJ-80948543 vs NullxCD20xCD3 ($p=0.0011$), JNJ-80948543 vs NullxNullxCD3 ($p<0.0001$); CARNAVAL cells JNJ-80948543 vs CD79bxNullxCD3 ($p<0.0001$), JNJ-80948543 vs NullxCD20xCD3 ($p=0.0018$), JNJ-80948543 vs NullxNullxCD3 ($p<0.0001$).

ANOVA, analysis of variance; CD, cluster of differentiation; E:T, effector to target ratio; SEM, standard error of the mean.

Figure 3. JNJ-80948543 mediates cytotoxicity of B-NHL cells with different CD79/CD20 expression levels.

(A) Effect of JNJ-80948543 and NullxNullxCD3 antibodies on cytotoxicity of B-NHL cells expressing CD79b and/or CD20 in the presence of T cells from healthy donors (n=5–7) at 5:1 E:T ratio. Cytotoxicity of tumor cell targets was measured after 48 or 72 hours. All cell lines used were $CD79b^+$ and/or $CD20^+$ except SU DHL-1 and K562, which are $CD79b^-CD20^-$. Data from 6 independent experiments were averaged and means ± SEM are graphed.

(B) Effect of JNJ-80948543 and NullxNullxCD3 antibodies on cytotoxicity of B-NHL cells expressing CD79b and/or CD20 in the presence of T cells from healthy donors (n=5–6) at 1:1 E:T ratio. Cytotoxicity of tumor cell targets was measured after 48 or 72 hours. All cell lines used were $CD79b^+$ and $CD20^+$. Data were averaged and means ± SEM are graphed.

Significance in activity between JNJ-80948543 and NullxNullxCD3 control antibody per time point was calculated using Two-way ANOVA and the Bonferroni multiple comparison test: *p<0.05, ** p<0.01, ****p<0.0001.

ANOVA, analysis of variance; B-NHL, B-cell non-Hodgkin lymphoma; CD, cluster of differentiation; E:T, effector-to-target; SEM, standard error of the mean.

Figure 4. JNJ-80948543 mediates T-cell activation in the presence of $CD79b^+$ $CD20^+$ B-NHL cells.

(A) The percentage of CD8 T-cell activation was determined by flow cytometry (Y axis) as percent of $CD25^+$ cells. CFSE-labeled cell lines were combined with $CD3^+$ pan T cells at a 5:1 E:T ratio for either 48 or 72 hours with increasing concentrations (X axis) of JNJ-

80948543 or NullxNullxCD3. Values are averages of 5 to 6 individual T-cell donors. All cell lines are $CD79b^{+}/CD20^{+}$ except SU-DHL-1 and K562, which are $CD79b^{-}/CD20^{-}$. As SU-DHL-1 secretes IL-2 and thus induces CD25 on T cells in the coculture system, for assessing % of CD25 on CD8 T cells gate has been set up relative to untreated wells with SU-DHL-1 and T cells. Graphing of data was done in GraphPad Prism 9. Data from 6 independent experiments were pooled and represented as mean ± SEM. Significance in activity between JNJ-80948543 and NullxNullxCD3 control antibody per time point was calculated using Two-way ANOVA and the Bonferroni multiple comparison test: *p<0.05, ** p<0.01, ****p< 0.0001.

(B) T cells from 5 or 6 healthy donors were tested in T cell redirection assays incubated with the indicated antibodies and $CD79b^{+}CD20^{+}$ CARNAVAL (top) and OCI-Ly10 (bottom) cells. The assay was conducted for 48 or 72 hours, at 5:1 E:T ratio. Supernatant was analyzed for inflammatory cytokines using MSD Proinflammatory kit (MSD K15049D). Representative graphs for IFNγ, IL-2 and TNFa are shown (data for other cytokines are shown in supplemental figures; Supplemental Figure 4B and C).

B-NHL, B cell non-Hodgkin lymphoma; CD, cluster of differentiation; CFSE, carboxyfluorescein succinimidyl ester; E:T, effector-to-target; IL, interleukin; IFNγ, interferon gamma; MSD, meso scale discovery; SEM, standard error of the mean; TNFa, tumor necrosis factor alpha; TNFγ, tumor necrosis factor gama.

Figure 5. JNJ-80948543 mediates B-NHL cell cytotoxicity and T-cell activation in whole blood setting. JNJ-80948543 mediates CD79b antagonistic activity.

(A–D) Whole blood from 6 healthy donors was tested in T-cell redirection assays with the indicated antibodies and $CD79b^{+}CD20^{+}$ target cell lines: CARNAVAL (A, C) or OCI-Ly10

(B, D). The percent cytotoxicity of cancer cells (A, B) or T-cell activation (C, D) was determined after 48 or 72 hours. The assay was conducted at an E:T ratio of 1:1 with respect to added tumor cells.

(E, F) The percent cytotoxicity of primary B cells (E) or T-cell activation (F) was assessed in the whole blood assay without added cancer cells. The E:T ratio for primary B cells ranged from 5:1 to 10:1. Data were averaged and means ± SEM are graphed.

(G) JNJ-80948543, CD79bxNullxCD3, NullxCD20xCD3 and NullxNullxCD3 antibodies were added at a range of concentrations to OCI-Ly10 cells for 24 hours to assess the effect on IL-10 secretion, as surrogate of NF-κB signaling inhibition downstream of CD79b. IL-10 levels were normalized to untreated control cells and expressed as percent.

(H) JNJ-80948543, CD79bxNullxCD3, NullxCD20xCD3 and NullxNullxCD3 antibodies were added at a range of concentrations to HBL-1 cells for 24 hours to assess the effect on IL-10 secretion, as surrogate of NF-κB signaling inhibition downstream of CD79b. IL-10 levels were normalized to untreated control cells and expressed as percent.

Significance in activity between JNJ-80948543 and NullxNullxCD3 control antibody per time point was calculated using Two-way ANOVA and the Bonferroni multiple comparison test: *$p<0.05$, ** $p<0.01$, ****$p< 0.0001$.

ANOVA, analysis of variance; B-NHL, B cell non-Hodgkin lymphoma; CD, cluster of differentiation; E:T, effector-to-target; IL, interleukin; NF-κB, nuclear factor kappa light chain enhancer of activated B cells; SEM, standard error of the mean.

Figure 6. Antitumor efficacy of JNJ-80948543 on CARNAVAL and OCI-Ly10 xenografts and its impact on xenograft's T-cell infiltration.

(A, B) T cell-humanized NSG mice injected SC with (A) CARNAVAL tumors or (B) OCI-Ly10 tumors were dosed IP with JNJ-80948543 at 1 and 5 mg/kg for CARNAVAL or at 3 and 10 mg/kg for OCI-Ly10 (dosing time frame is denoted by bar below the X axis). Tumor volume was measured twice weekly and results presented as the mean tumor volume ± SEM for each group (n=10/group). Data are displayed while at least 2/3 of animals remained in a group. * Denotes significant difference ($p \leq 0.05$) compared with the DPBS control evaluated using a mixed model for repeated measures.

(C) Effect of JNJ-80948543 on $CD8^+$ T-cell Infiltration in SC OCI-Ly10 DLBCL tumors grown in T-cell-humanized mice. Tumor cells were implanted on Day 0, T cells were injected on Day 20, and dosing occurred on Days 21, 24, 27, and 31. Tumor samples were collected for analysis at 4, 24, 72, 96, and 168 hours post fourth dose (3 tumors per treatment group). Representative IHC micrographs are shown after staining for human CD8. (C1) Tumor treated with DPBS (vehicle) 4 hours post fourth dose; (C2, C3, C4) tumors treated with JNJ-80948543 at 3 mg/kg at 4, 72, and 168 hours post fourth dose, respectively; (C1–C4) scanned at 40× magnification. (C5 and C6) Higher magnifications of tumors treated with DPBS or JNJ-80948543 at 3 mg/kg at 4 hours post dose, respectively. Magnification bars represent 1 mm (C1–C4) and 100 µm (C5 and C6).

CD, cluster of differentiation; DLBCL, diffuse large B-cell lymphoma; DPBS, Dulbecco's phosphate-buffered saline; IHC, immunohistochemistry, IP, intraperitoneal; SC, subcutaneous; SEM, standard error of the mean.

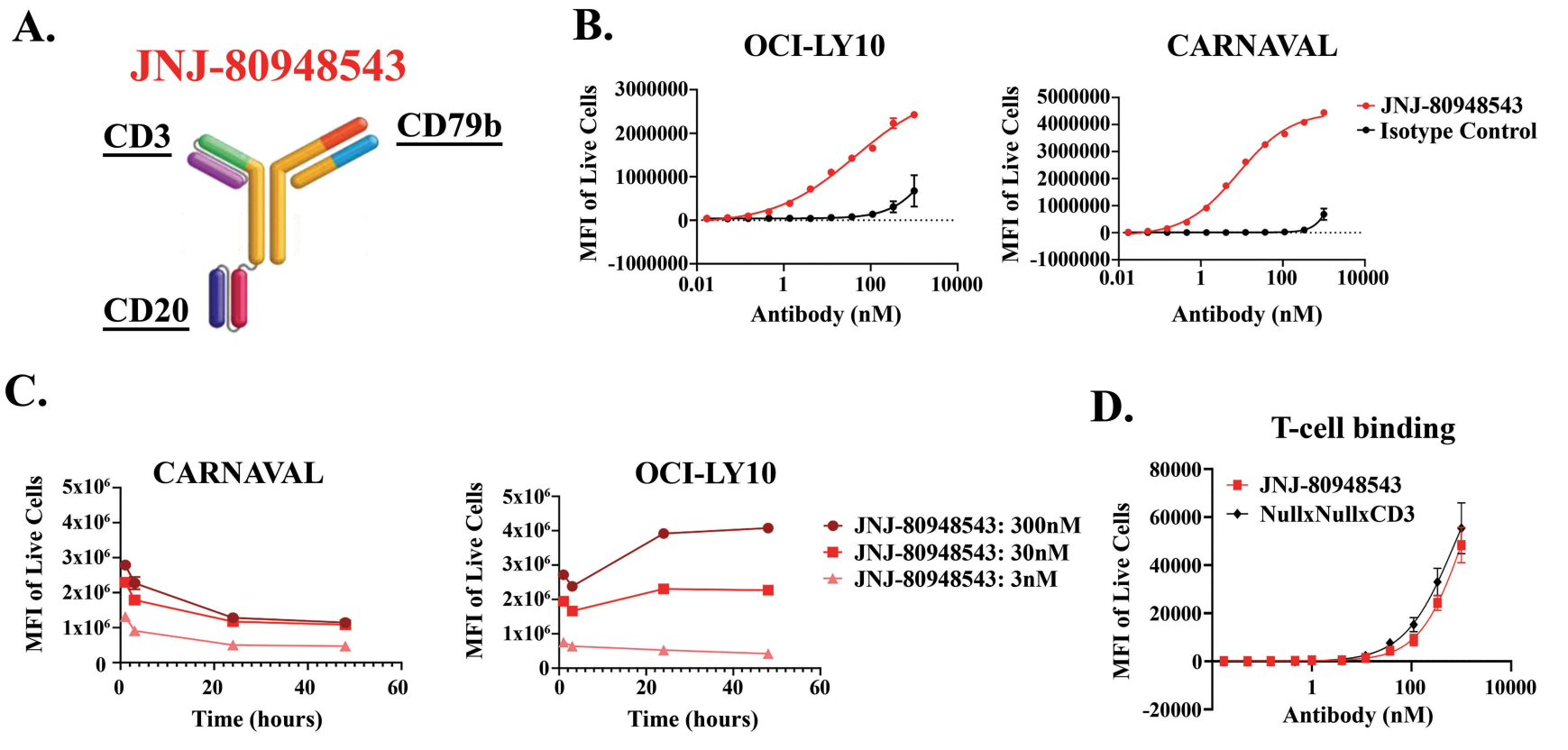
A.
JNJ-80948543
CD3
CD79b
CD20
B.
OCI-LY10
MFI of Live Cells
3000000
2000000
1000000
0
-1000000
0.01
1
100
10000
Antibody (nM)
CARNAVAL
MFI of Live Cells
5000000
4000000
3000000
2000000
1000000
0
-1000000
0.01
1
100
10000
Antibody (nM)
JNJ-80948543
Isotype Control
C.
CARNAVAL
MFI of Live Cells
5x10⁶
4x10⁶
3x10⁶
2x10⁶
1x10⁶
0
0
20
40
60
Time (hours)
OCI-LY10
MFI of Live Cells
5x10⁶
4x10⁶
3x10⁶
2x10⁶
1x10⁶
0
0
20
40
60
Time (hours)
JNJ-80948543: 300nM
JNJ-80948543: 30nM
JNJ-80948543: 3nM
D.
T-cell binding
MFI of Live Cells
80000
60000
40000
20000
0
-20000
1
100
10000
Antibody (nM)
JNJ-80948543
NullxNullxCD3

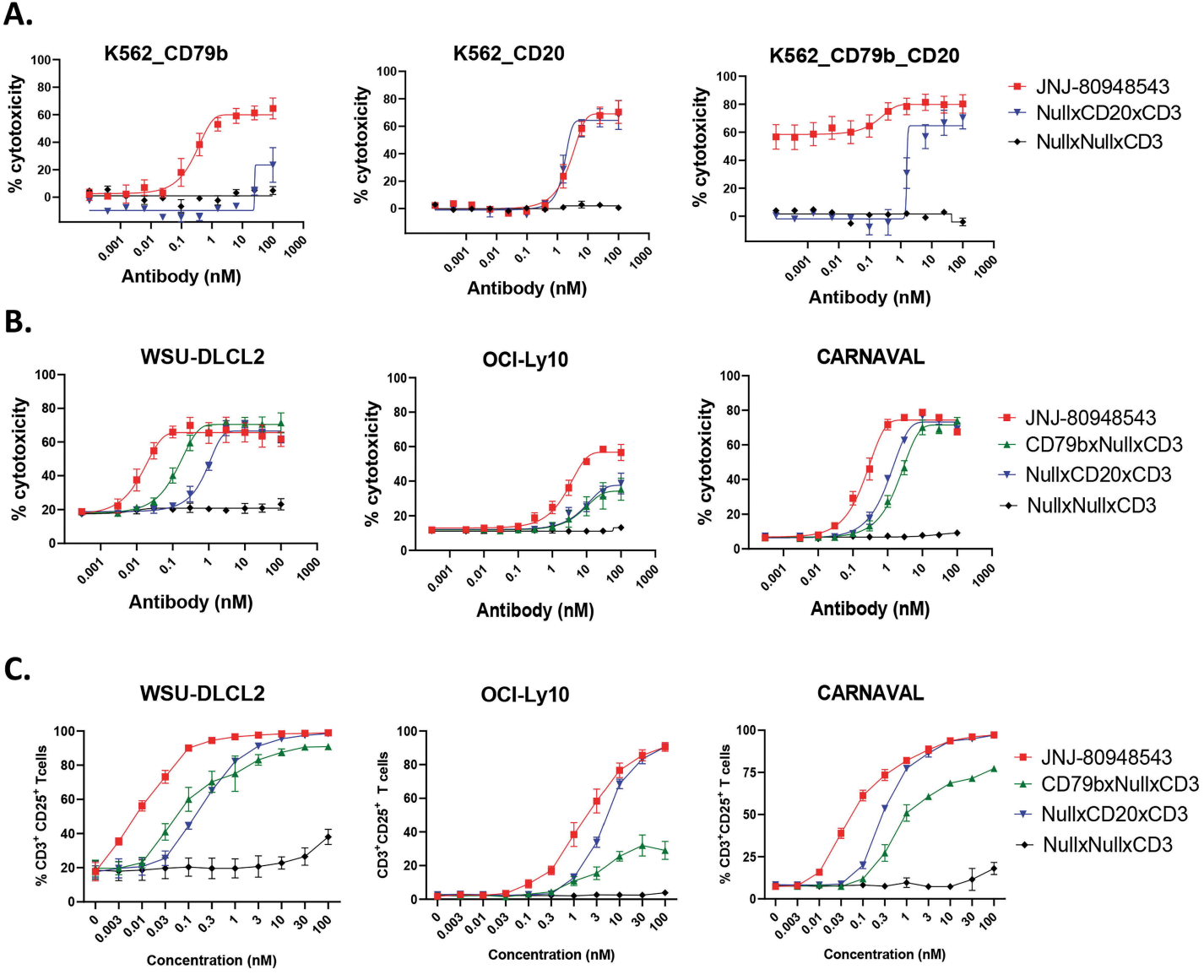
A.
K562_CD79b
K562_CD20
K562_CD79b_CD20
% cytotoxicity
Antibody (nM)
JNJ-80948543
NullxCD20xCD3
NullxNullxCD3
B.
WSU-DLCL2
OCI-Ly10
CARNAVAL
% cytotoxicity
Antibody (nM)
JNJ-80948543
CD79bxNullxCD3
NullxCD20xCD3
NullxNullxCD3
C.
WSU-DLCL2
OCI-Ly10
CARNAVAL
% CD3+ CD25+ Tcells
CD3+CD25+ T cells
Concentration (nM)
JNJ-80948543
CD79bxNullxCD3
NullxCD20xCD3
NullxNullxCD3

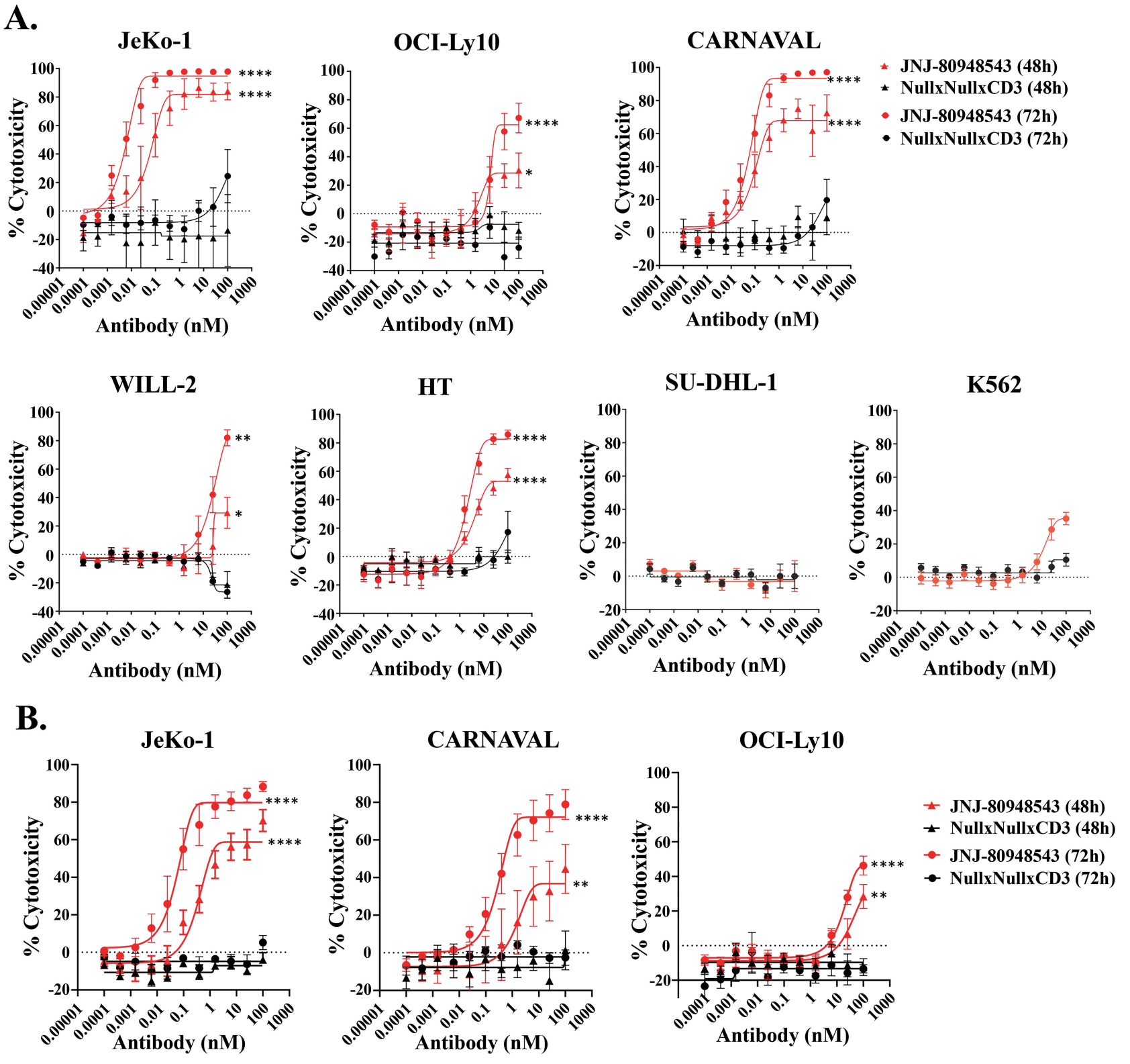
A.
JeKo-1
OCI-Ly10
CARNAVAL
WILL-2
HT
SU-DHL-1
K562
% Cytotoxicity
Antibody (nM)
JNJ-80948543 (48h)
NullxNullxCD3 (48h)
JNJ-80948543 (72h)
NullxNullxCD3 (72h)
B.
JeKo-1
CARNAVAL
OCI-Ly10
% Cytotoxicity
Antibody (nM)
JNJ-80948543 (48h)
NullxNullxCD3 (48h)
JNJ-80948543 (72h)
NullxNullxCD3 (72h)

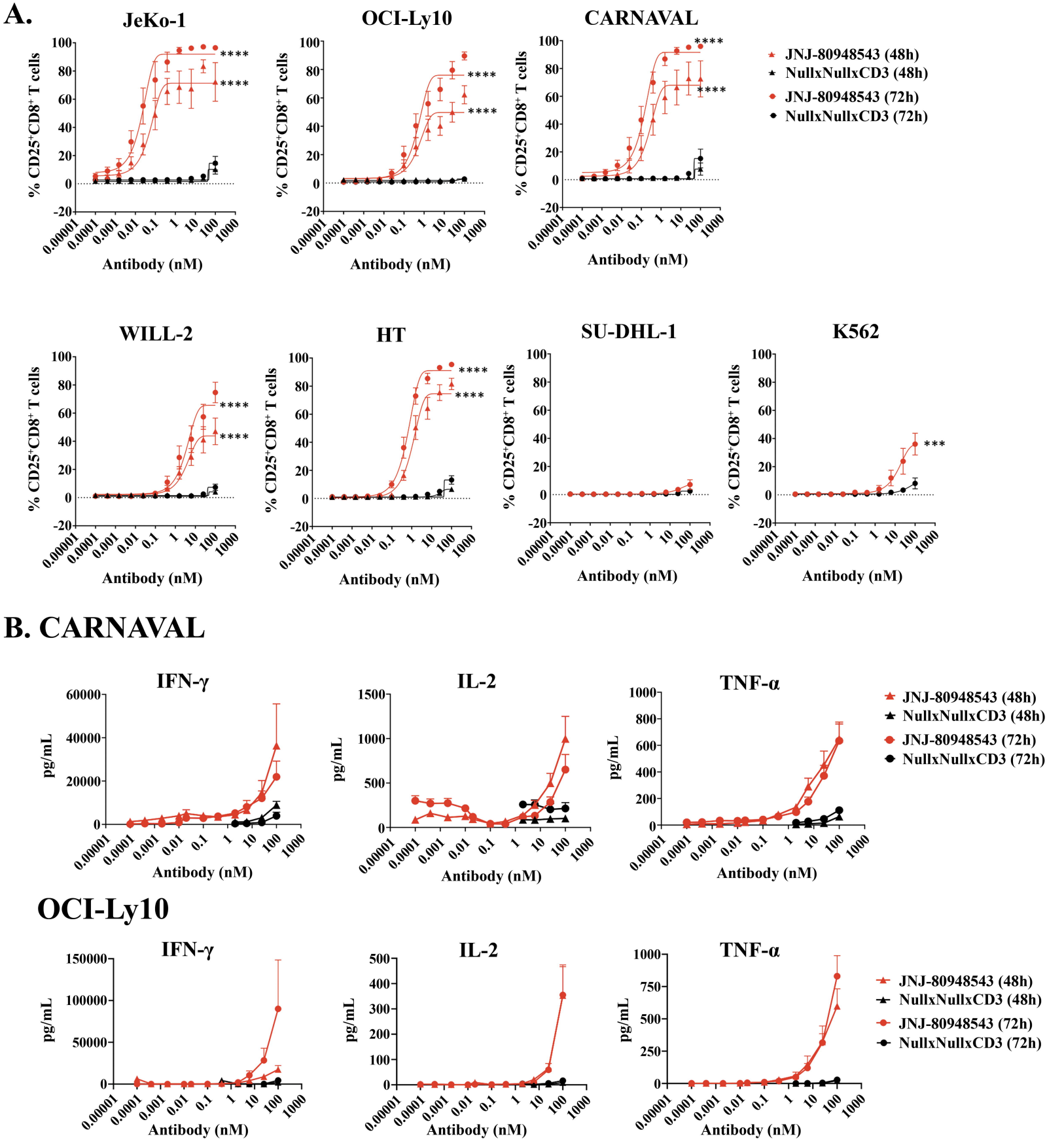
A.
JeKo-1
OCI-Ly10
CARNAVAL
WILL-2
HT
SU-DHL-1
K562
% CD25+CD8+ T cells
Antibody (nM)
JNJ-80948543 (48h)
NullxNullxCD3 (48h)
JNJ-80948543 (72h)
NullxNullxCD3 (72h)
B. CARNAVAL
IFN-γ
IL-2
TNF-α
pg/mL
OCI-Ly10

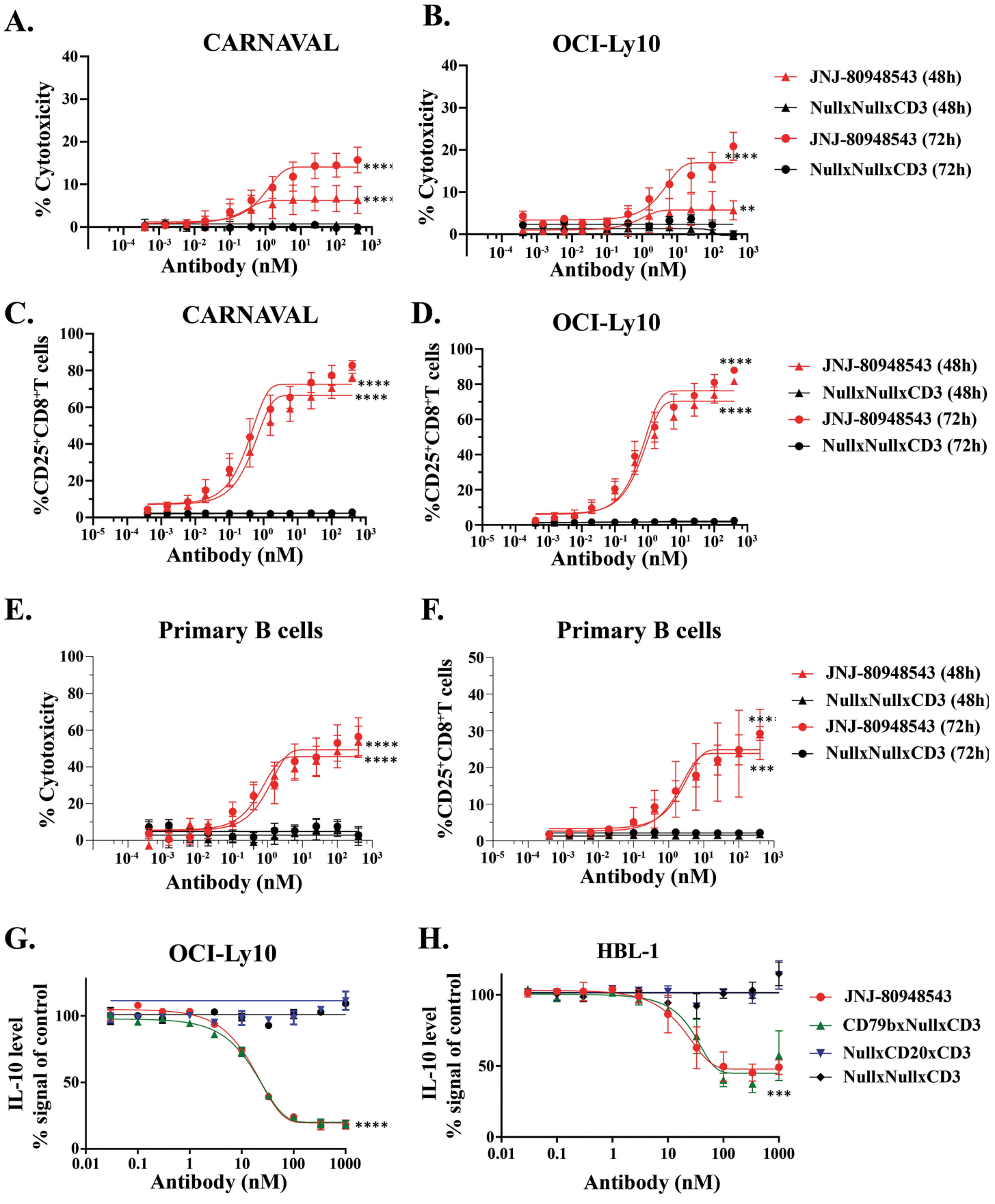
A.
CARNAVAL
% Cytotoxicity
Antibody (nM)
B.
OCI-Ly10
% Cytotoxicity
Antibody (nM)
JNJ-80948543 (48h)
NullxNullxCD3 (48h)
JNJ-80948543 (72h)
NullxNullxCD3 (72h)
C.
CARNAVAL
%CD25+CD8+T cells
Antibody (nM)
D.
OCI-Ly10
%CD25+CD8+T cells
Antibody (nM)
JNJ-80948543 (48h)
NullxNullxCD3 (48h)
JNJ-80948543 (72h)
NullxNullxCD3 (72h)
E.
Primary B cells
% Cytotoxicity
Antibody (nM)
F.
Primary B cells
%CD25+CD8+T cells
Antibody (nM)
JNJ-80948543 (48h)
NullxNullxCD3 (48h)
JNJ-80948543 (72h)
NullxNullxCD3 (72h)
G.
OCI-Ly10
IL-10 level
% signal of control
Antibody (nM)
H.
HBL-1
IL-10 level
% signal of control
Antibody (nM)
JNJ-80948543
CD79bxNullxCD3
NullxCD20xCD3
NullxNullxCD3

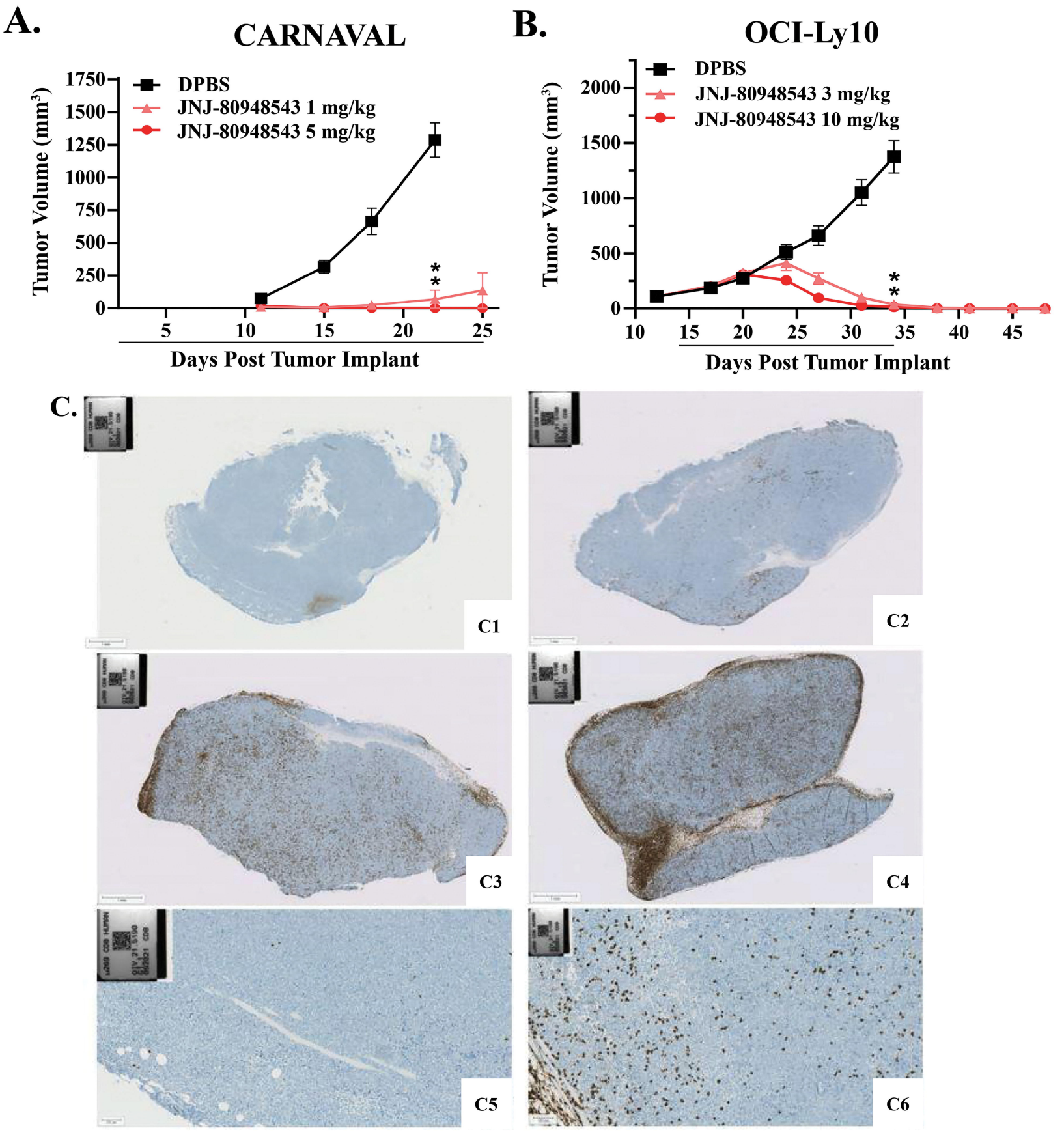
A.
CARNAVAL
Tumor Volume (mm3)
1750
1500
1250
1000
750
500
250
0
DPBS
JNJ-80948543 1 mg/kg
JNJ-80948543 5 mg/kg
**
5
10
15
20
25
Days Post Tumor Implant
B.
OCI-Ly10
Tumor Volume (mm3)
2000
1500
1000
500
0
DPBS
JNJ-80948543 3 mg/kg
JNJ-80948543 10 mg/kg
**
10
15
20
25
30
35
40
45
Days Post Tumor Implant
C.
C1
C2
C3
C4
C5
C6

[Supplemental Data]

Supplemental Table 1. CD79b and CD20 antigen density in hematologic tumor cell lines

Cell line	Cell line origin	CD79b ABC*	CD20 ABC*
CARNAVAL	DLBCL	220,000	250,000
OCI-Ly10	DLBCL	115,000	230,000
JeKo1	MCL	760,000	225,000
WILL2	DLBCL	7,200	1,200
HT	DLBCL	0	21,000
SUDHL1	ALCL	0	0
K562	CML	0	0

*ABC values are rounded and represent the results of 3 independent experiments.

ABC, antibody binding capacity; ALCL, anaplastic large cell lymphoma; CD, cluster of differentiation; CML, chronic myeloid leukemia; DLBCL, diffuse large B cell lymphoma; MCL, mantle cell lymphoma.

Supplemental Table 2. Cytotoxicity EC_{50} and maximum values observed for JNJ-80948543, CD79bxNullxCD3, NullxCD20xCD3 in T cell cytotoxicity assays conducted with tumor targets expressing CD79b and/or CD20 at 5:1 E:T ratios

OCI-Ly10 (72 hours)			
	JNJ-80948543	**CD79bxNullxCD3**	**NullxCD20xCD3**
EC_{50} (nM)	2.615	8.435	11.28
Max kill (%)	59.7%	37.0%	43.3%
CARNAVAL (72hours)			
EC_{50} (nM)	0.1973	1.972	0.9805
Max kill (%)	75.4%	74.0%	73.8%
WSU-DLCL2 (72hours)			
EC_{50} (nM)	0.0132	0.1285	0.7679
Max kill (%)	65.7%	71.2%	67.0%

EC_{50}, 50% effective concentration; E:T, effector to target; Max kill, maximum cytotoxicity;

T cell cytotoxicity assays were conducted using JNJ-80948543, CD79bxNullxCD3, NullxCD20xCD3, T cells derived from 3 healthy donors, and target cell lines expressing CD79b and/or CD20, for 72 hours. Data from 3 independent experiments were pooled and represented as means. EC_{50} was calculated using [inhibitor] vs. response – variable slope (four parameters) with GraphPad.

Supplemental Table 3. Cytotoxicity EC_{50} and maximum values observed for JNJ-80948543 in T cell cytotoxicity assays conducted with tumor targets expressing CD79b and/or CD20 at 5:1 and 1:1 E:T ratios

48 hours (means)					
	JeKo1	**CARNAVAL**	**OCILy10**	**HT**	**WILL2**
5:1					
EC_{50} (nM)	0.149	0.237	2.221	4.186	NE
Max kill (%)	90.8	78.4	31.0	59.1	NE
1:1					
EC_{50} (nM)	0.588	0.658	94.462[a]	NA	NA
Max kill (%)	65.8	35.0	62.8[a]	NA	NA
72 hours (means)					
	JeKo1	**CARNAVAL**	**OCILy10**	**HT**	**WILL2**
5:1					
EC_{50} (nM)	0.0092	0.092	27.042	2.016	31.971
Max kill (%)	99.0	98.5	81.8	86.8	95.5
1:1					
EC_{50} (nM)	0.155	0.536	16.543	NA	NA
Max kill (%)	85.9	77.8	49.3	NA	NA

EC_{50}, 50% effective concentration; E:T, effector to target; Max kill, maximum cytotoxicity; NA, not assessed; NE, not estimable.

T cell cytotoxicity assays were conducted using JNJ-80948543, T cells derived from 5 to 7 healthy donors, and target cell lines expressing CD79b and/or CD20, for 48 or 72 hours. Data from 6 independent experiments were pooled and represented as means.

[a]High variability across tested donors.

Supplemental Table 4: Cytokine Secretion EC_{50} (nM) and Maximum Values (pg/mL) Observed for JNJ-80948543 in T-cell Redirection Assays Conducted with CARNAVAL and OCI-Ly10 Cells at 5:1 and 1:1 E:T Ratios.

	48 hours				72 hours			
	CARNAVAL		OCI-Ly10		CARNAVAL		OCI-Ly10	
	E:T ratio							
	1:1	5:1	1:1	5:1	1:1	5:1	1:1	5:1
IFN-γ								
EC_{50}	2.097	NE	36.339	55.646	1.571	48.338	13.744	85.887
Max value	4,213.3	NE	5,630.8	16,564.2	12,185.5	30,242.4	16,383.0	59,934.1
IL-1β								
EC_{50}	NE	NE	ND	ND	NE	NE	ND	ND
Max value	NE	NE	ND	ND	NE	NE	ND	ND
IL-2								
EC_{50}	2.871	15.516	62.195	>100[a]	>100[a]	>100[a]	>100[a]	>100[a]
Max value	386.8	747.7	105.0	461.7	1,005.3	1,468.5	0.1	1,253.9
IL-4								
EC_{50}	1.894	7.946	NE	NE	14.044	37.367	NE	NE
Max value	2.1	11.1	NE	NE	3.0	11.1	NE	NE
IL-8								
EC_{50}	NE	NE	15.050	1.944	NE	NE	>100[a]	1.878
Max value	NE	NE	5.3	19.1	NE	NE	23.2	32.8
IL-6								
EC_{50}	NE	NE	1.251	NE	NE	NE	8.545	NE
Max value	NE	NE	5.5	NE	NE	NE	17.1	NE
IL-10								
EC_{50}	1.047	>100[a]	NE	NE	0.939	>100[a]	NE	NE
Max value	81.0	1,173.8	NE	NE	67.2	223,016.3	NE	NE
IL-13								
EC_{50}	0.429	3.392	NE	NE	0.202	17.497	NE	NE
Max value	0.2	42.5	NE	NE	42.9	77.3	NE	NE
TNF-α								
EC_{50}	2.158	60.226	>100[a]	>100[a]	10.573	>100[a]	33.971	>100[a]
Max value	282.0	980.4	234.6	1,310.3	397.0	2,382.7	344.8	3,143.2

CD, cluster of differentiation; EC_{50}, 50% effective concentration; E:T, effector to target; IFN, interferon; IL, interleukin; Max value, maximal cytokine release value; ND; not detectable; NE, not estimable; TNF, tumor necrosis factor.

T cells from 5 or 6 healthy donors were tested in T-cell redirection assays, incubated with JNJ-80948543 and $CD79b^{+}CD20^{+}$ CARNAVAL or OCI-Ly10 cells. The assay was conducted for 48 or 72 hours, with a single point per condition and donor. Supernatants were tested for the presence of cytokines. EC_{50} values could not be estimated for cytokines for which non-sigmoidal or decreasing response was observed and were listed in the table as NE. Data from 6 independent experiments are averaged and mean value reported.

[a] EC_{50} value estimated to be higher than highest tested concentration.

Supplemental Figure 1. JNJ-80948543 Antigen Specific T-Cell Activation Dependent Cytokine Release

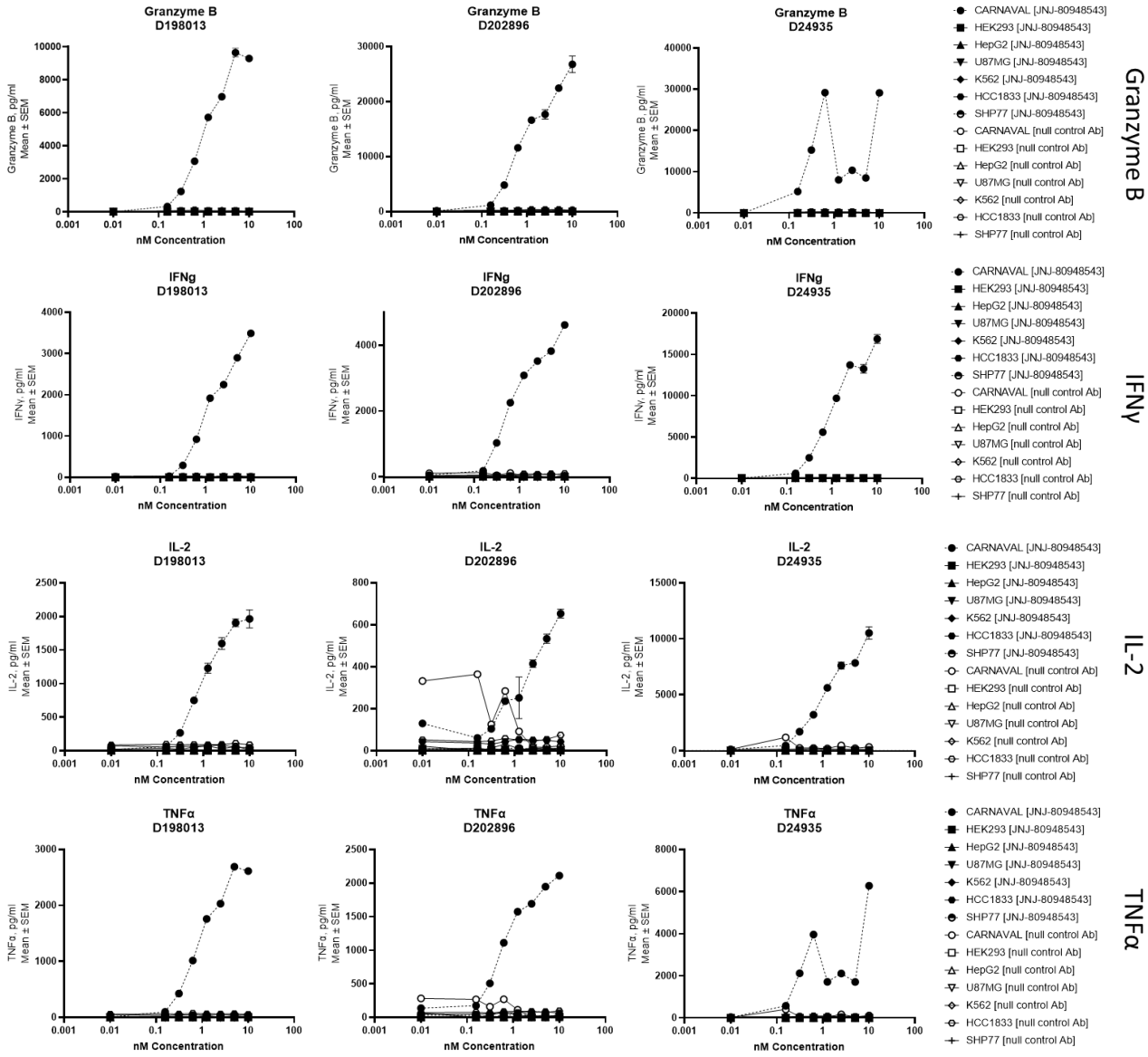

Primary T cells from 3 healthy donors (D198013, D202896, and D24935) were co-cultured with individual CD79b and CD20 antigen negative cell lines (HEK-293T, K562, HCC-1833, HepG2, U87MG and SHP-77) and an antigen positive control cell line (CARNAVAL, circle). Cells were treated with a titration of JNJ-80948543 (filled shapes) and null control Ab (open shapes). Supernatants were harvested at t=72hrs post-treatment and assessed for cytokines (Granzyme B, IFNγ, TNFα and IL-2) as a measure of antibody-induced T-cell activation. Technical replicates (n=3) were averaged and the mean ± SEM were plotted.

Supplemental Figure 2. CD79b and CD20 expression in B-NHL patient samples compared with patients with lymphadenitis or healthy donor B cells

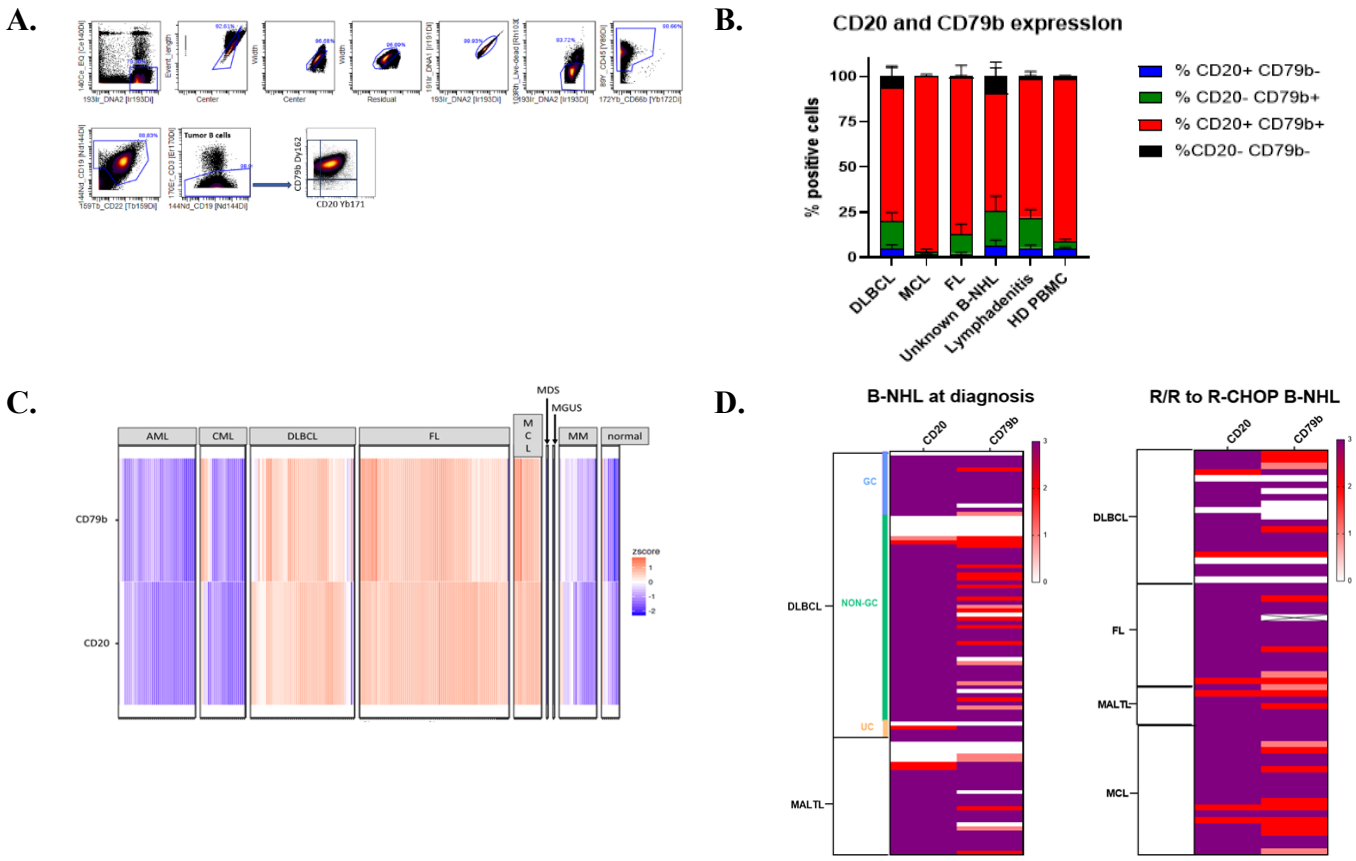

(A) Exemplary hierarchical gating strategy for identification of tumor B cells in lymph node biopsies from patients with newly diagnosed B-NHL. Tumor B cells were defined as $CD45^{+}CD66b^{-}CD19^{+}CD22^{all}CD3^{-}$ (following the exclusion of debris, dead cells and doublets). $CD79b^{+}CD20^{+}$, $CD79b^{-}CD20^{+}$, $CD79b^{-}CD20^{-}$ and $CD79b^{+}CD20^{-}$ were identified within the tumor B cells.

(B) Dissociated lymph node tissues from treatment-naïve B-NHL patients (DLBC: n=6; FL: n=3; MCL: n=7; unknown B-NHL: n=5) and patients with lymphadenitis (n=7) or healthy donor peripheral blood mononuclear cells (n=9) were stained with Maxpar Direct Immune Profiling Assay antibody cocktail supplemented with anti-CD79b antibody to determine CD79b and CD20 expression in the B-cell lineage cell by CyTOF.

C) InforMe database was used to quantitate the relative mRNA levels of CD79b and CD20 across hematological malignancies using the GeneLogic Heme Plus 2.0 data set. mRNA levels are expressed as z scores, which describes the expression of a gene relative to the average across all of the samples. This analysis included n=226 samples obtained from tumor tissues: acute myeloid leukemia (AML; n=39), CML (n=23), DLBCL (n=53), FL (n=76), MCL (n=14), multiple myeloma (MM) (n=19), myelodysplastic syndrome (MDS; n=1), monoclonal gammopathy of undetermined significance (MGUS; n=1), and non-malignant non-lymphoid tissue control samples collected from patients (n=9; DLBCL [n=4], FL [n=3], MCL [n=2]).

(D) CD79b and CD20 IHC staining were performed on TMAs from B NHL patients at diagnosis or on FFPE samples from R/R to R-CHOP-treated B NHL patients. Staining intensity and utilizing scores (0, 1+, 2+, or 3+) are represented as a heat map and used for data visualization. In cases where range of intensity was provided, the more conservative (lower)

value was used for representation. Each row represents a single sample. A sample from the FL group could not be scored for CD79b due to tissue loss during IHC (crossed out). Samples at diagnosis consisted of n=28 MALTL samples, n=72 DLBCL samples. R/R lymphoma patient samples consisted of n=7 MALTL samples, n=21 DLBCL samples, n=16 FL samples, and n=20 MCL samples.

AML, acute myeloid leukemia; B-NHL, B cell non-Hodgkin lymphoma; CD, cluster of differentiation; CML, chronic myeloid leukemia; DLBCL, diffuse large B cell lymphoma; FFPE, formalin-fixed, paraffin-embedded; FL, follicular lymphoma; GC, germinal center; IHC, immunohistochemistry; MALTL, mucosa-associated lymphoid tissue lymphoma; MCL, mantle cell lymphoma; MDS, myelodysplastic syndrome; MGUS, monoclonal gammopathy of undetermined significance; MM, multiple myeloma; RCHOP, rituximab – cyclophosphamide – hydroxydaunorubicin – oncovin – prednisone/prednisolone; R/R, relapsed/refractory; TMA, tissue microarray; UC, uncharacterized for GC or NON-GC.

Supplemental Figure 3. Binding and in vitro functional characterization of JNJ-80948543

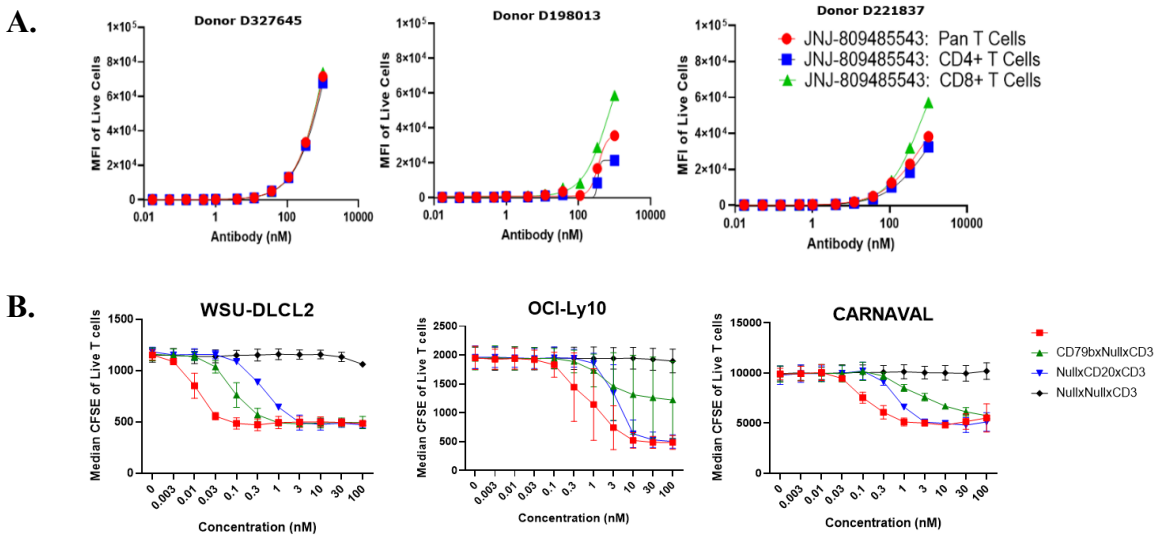

(A) Binding of JNJ-80948543 to primary T cell from 3 donors after 1 hour 37°C incubation. CD3, CD4 and CD8 T cell populations were assessed. Single data per point. Experiment was performed once with 3 T cell donors.

(D) T-cell proliferation was assessed in the presence of JNJ-80948543, CD79bxNullxCD3, NullxCD20xCD3, and NullxNullxCD3 antibodies and WSU-DLCL2, OCI-Ly10, CARNAVAL tumor cells and T cells from healthy donors at 5:1 E:T ratio. T-cell proliferation was assessed by flow cytometry using median CFSE decay as readout. Data from 3 independent experiments, 1 T cell donor per experiment are graphed as mean± SEM (n=3).

Supplemental Figure 4. JNJ-80948543 effect on T-cell activation in the presence of $CD79b^+$ $CD20^+$ B-NHL tumor cells in vitro

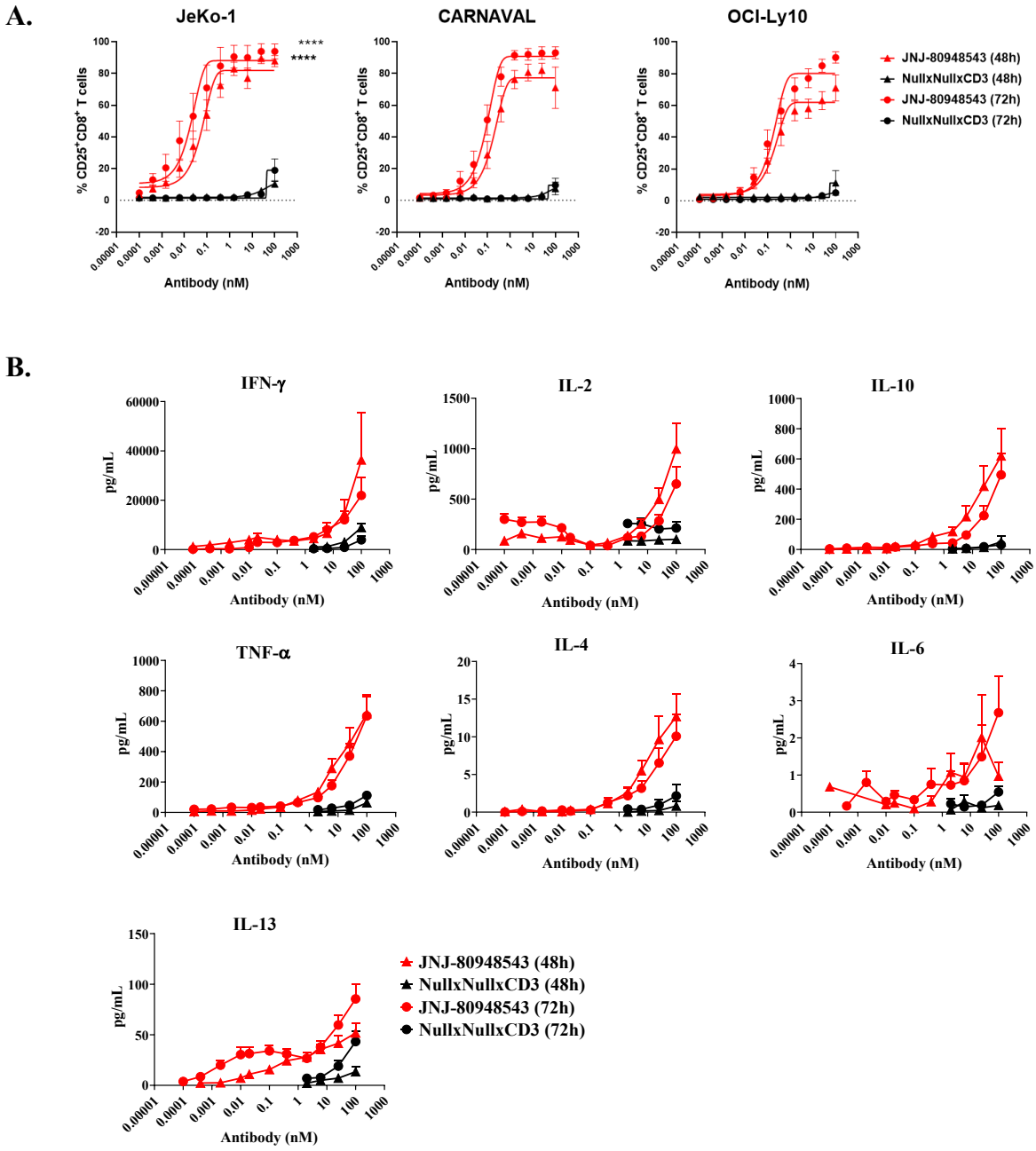

C.

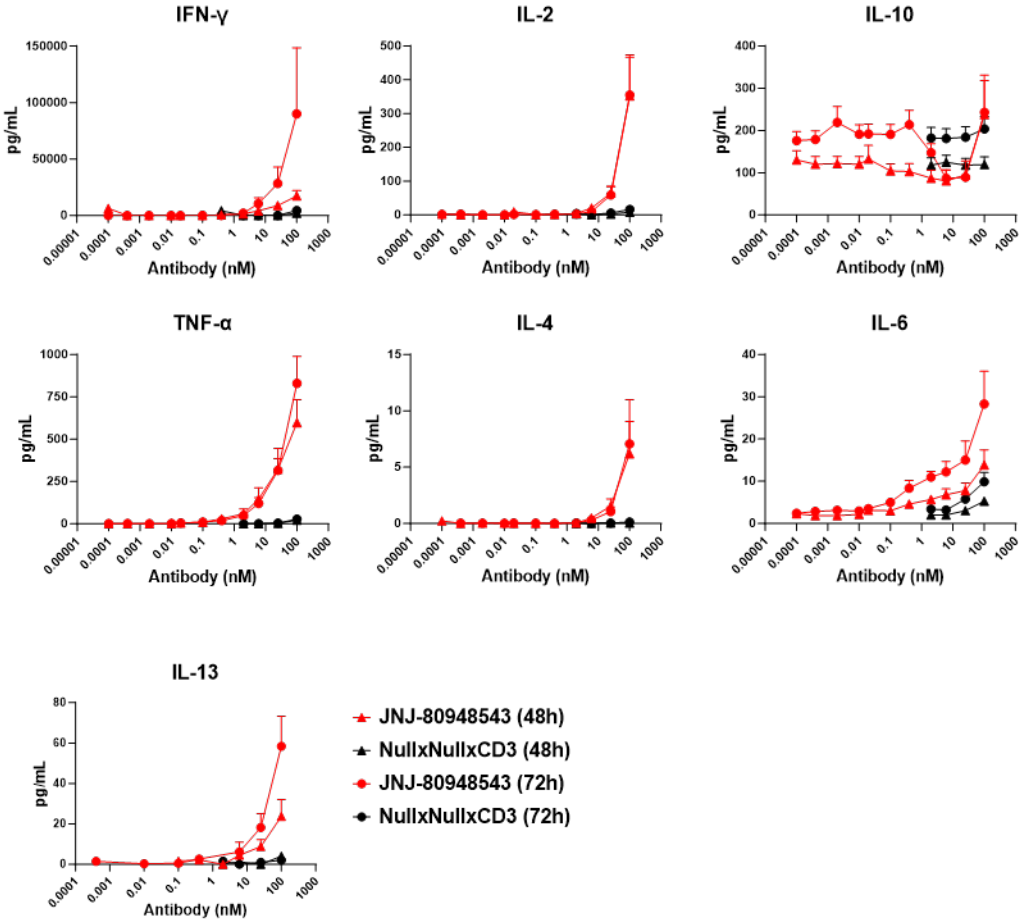

(A) The percentage of CD8 T-cell activation was determined by flow cytometry (Y axis) as percent of $CD25^+$ cells. Cancer cell lines were combined with $CD3^+$ pan T cells at a 1:1 effector-to-target ratio for either 48 or 72 hours with increasing concentrations (X axis) of JNJ-80948543 or NullxNullxCD3. Values are averages of 5 to 6 individual T cell donors. All cell lines are $CD79b^+/CD20^+$. Data from 6 independent experiments were pooled and represented as mean ± SEM (n=5-6).

(B) T cells from 5 or 6 healthy donors were tested in T cell redirection assays incubated with the indicated antibodies and $CD79b^+CD20^+$ CARNAVAL cells. The assay was conducted for 48 or 72 hours, at 5:1 E:T ratio. Supernatant was analyzed for inflammatory cytokines using MSD Proinflammatory kit (MSD K15049D). Data from 6 independent experiments are graphed as mean± SEM (n=5-6).

(C) T cells from 5 or 6 healthy donors were tested in T cell redirection assays incubated with the indicated antibodies and $CD79b^+CD20^+$ OCI-Ly10 cells. The assay was conducted for 48 or 72 hours, at 5:1 E:T ratio. Supernatant was analyzed for inflammatory cytokines using MSD Proinflammatory kit (MSD K15049D). Data are graphed as from 6 independent experiments mean± SEM (n=5-6).

Supplemental Figure 5. JNJ-80948556 profiling for binding to cancer cells and T cells and profiling for cytokine secretion

A. **JNJ-80948556** (higher affinity CD3)

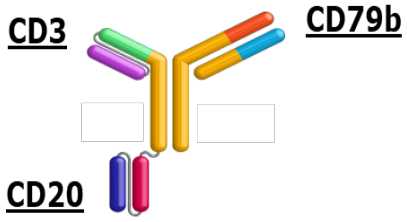

B.

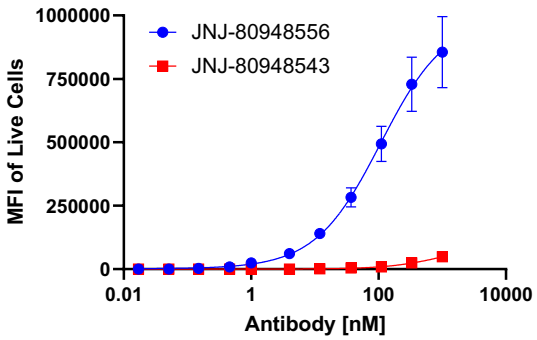

C.

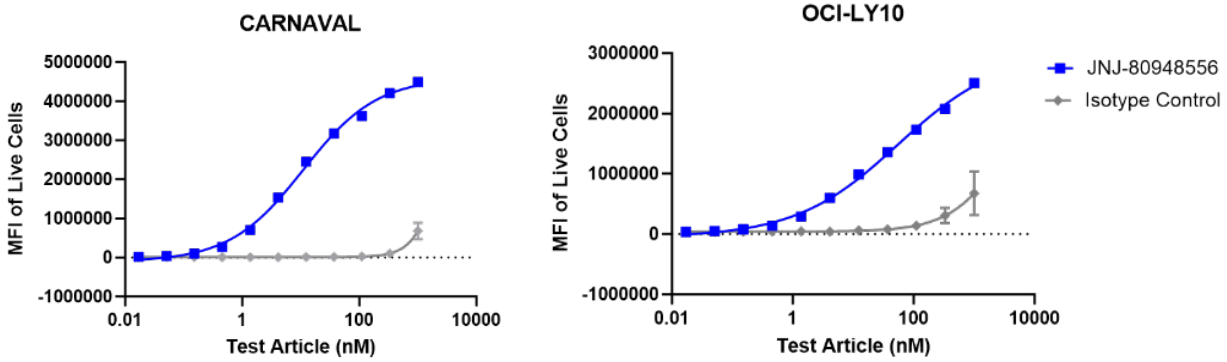

D.

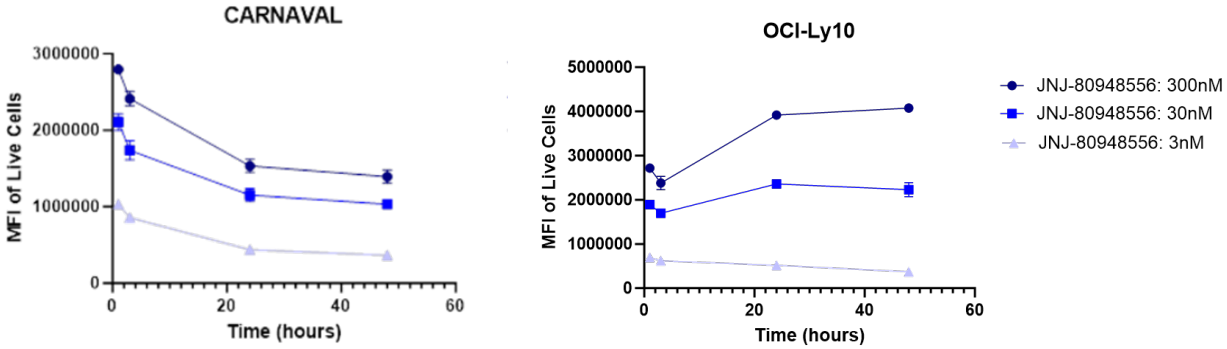

E.

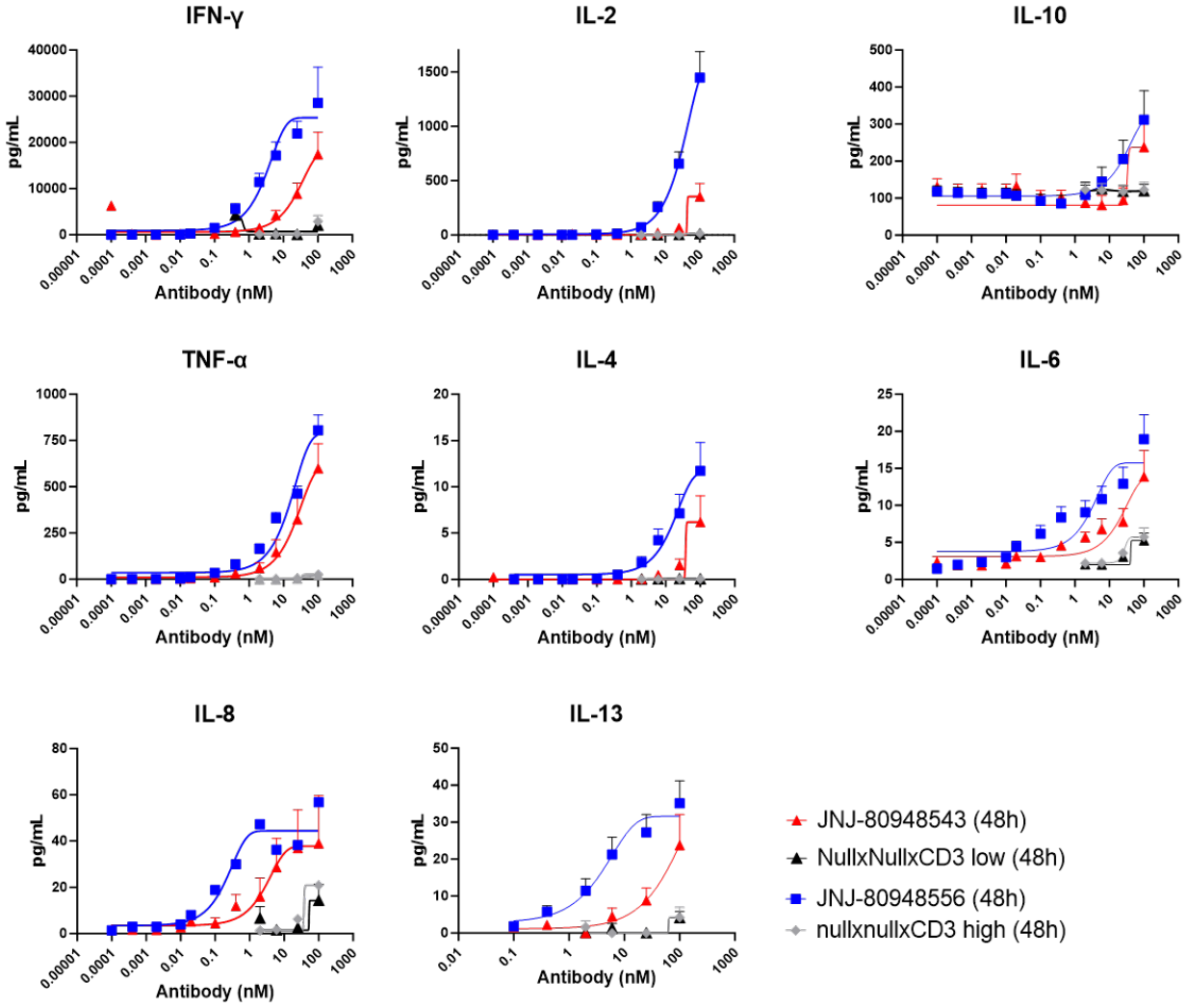
IFN-γ
IL-2
IL-10
TNF-α
IL-4
IL-6
IL-8
IL-13
pg/mL
Antibody (nM)
JNJ-80948543 (48h)
NullxNullxCD3 low (48h)
JNJ-80948556 (48h)
nullxnullxCD3 high (48h)

F.

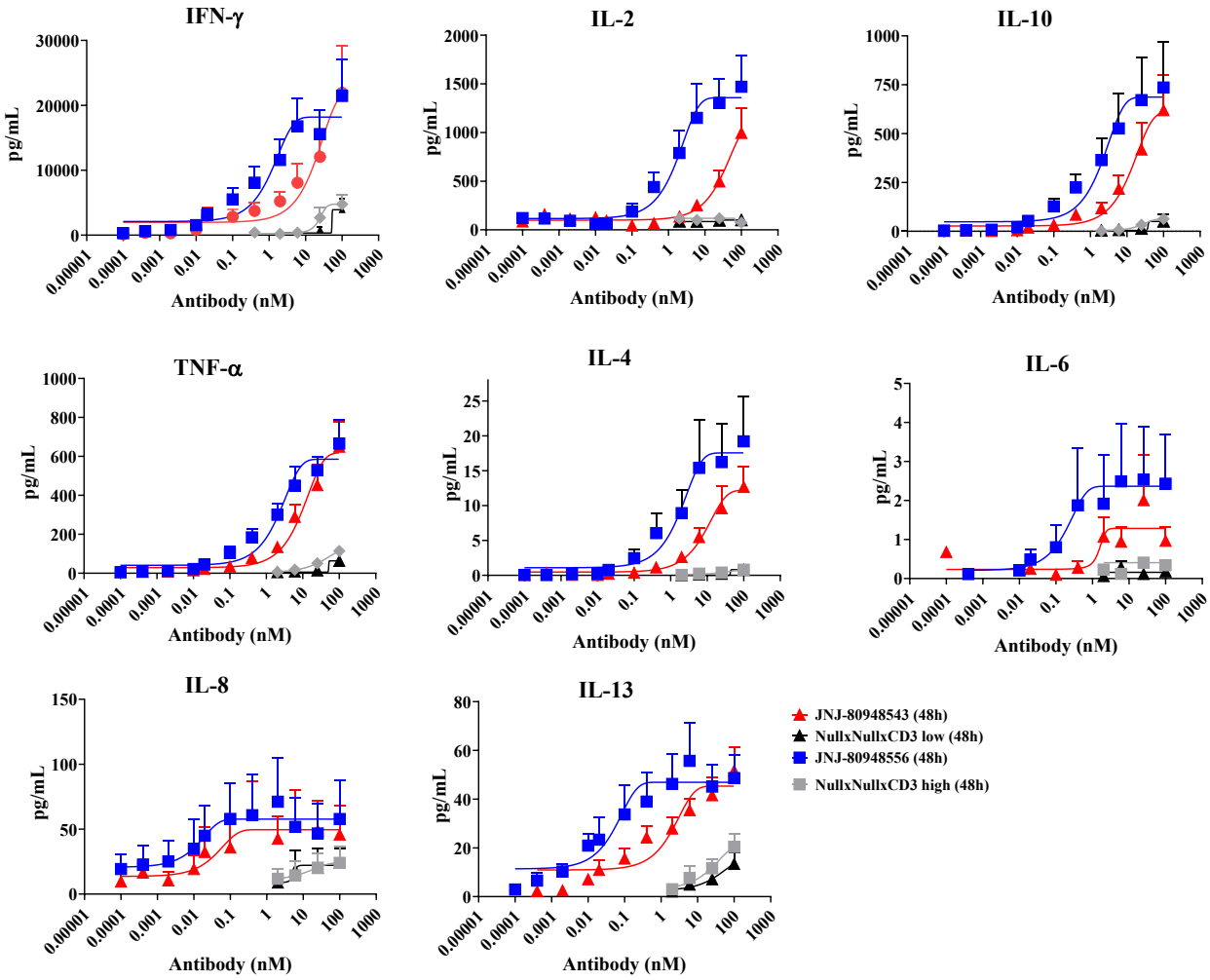

(A) JNJ-80948556 trispecific antibody schematic.

(B) Binding of JNJ-80948543 and JNJ-80948556 to primary T cell from 3 donors after 1 hour 37°C incubation. Data from single experiment are graphed as mean± SEM (n= 3).

(C) Dose-dependent binding of JNJ-80948556 to CARNAVAL and OCI-Ly10 B-NHL cells at 1 hour. Data from two independent experiments are graphed as mean± SEM (n= 2 replicates).

(D) Binding of JNJ-80948556 over time (up to 48h) to CARNAVAL and OCI-Ly10 B-NHL cells. Data from two independent experiments are graphed as mean± SEM (n= 2 replicates).

(E) T cells from 5 or 6 healthy donors were tested in T cell redirection assays incubated with the indicated antibodies and $CD79b^{+}CD20^{+}$ OCI-Ly10 cells. The assay was conducted for 48 hours, at 5:1 E:T ratio. Supernatant was analyzed for inflammatory cytokines using MSD Proinflammatory kit (MSD K15049D). Data from 6 independent experiments are graphed as mean± SEM (n=5-6).

(F) T cells from 5 healthy donors were tested in T cell redirection assays incubated with the indicated antibodies and $CD79b^{+}CD20^{+}$ CARNAVAL cells. The assay was conducted for 48 or 72 hours, at 5:1 E:T ratio. Supernatant was analyzed for inflammatory cytokines using MSD Proinflammatory kit (MSD K15049D). Data from 5 independent experiments are graphed as mean± SEM (n=5).

Supplemental Figure 6. Effect of JNJ-80948543 on primary B-Cell cytotoxicity or Cytokine Induction in Whole-blood T-cell Redirection Assays, Conducted at 1:1 E:T Ratio in the Presence or absence of CARNAVAL or OCI-Ly10 Cells

A.

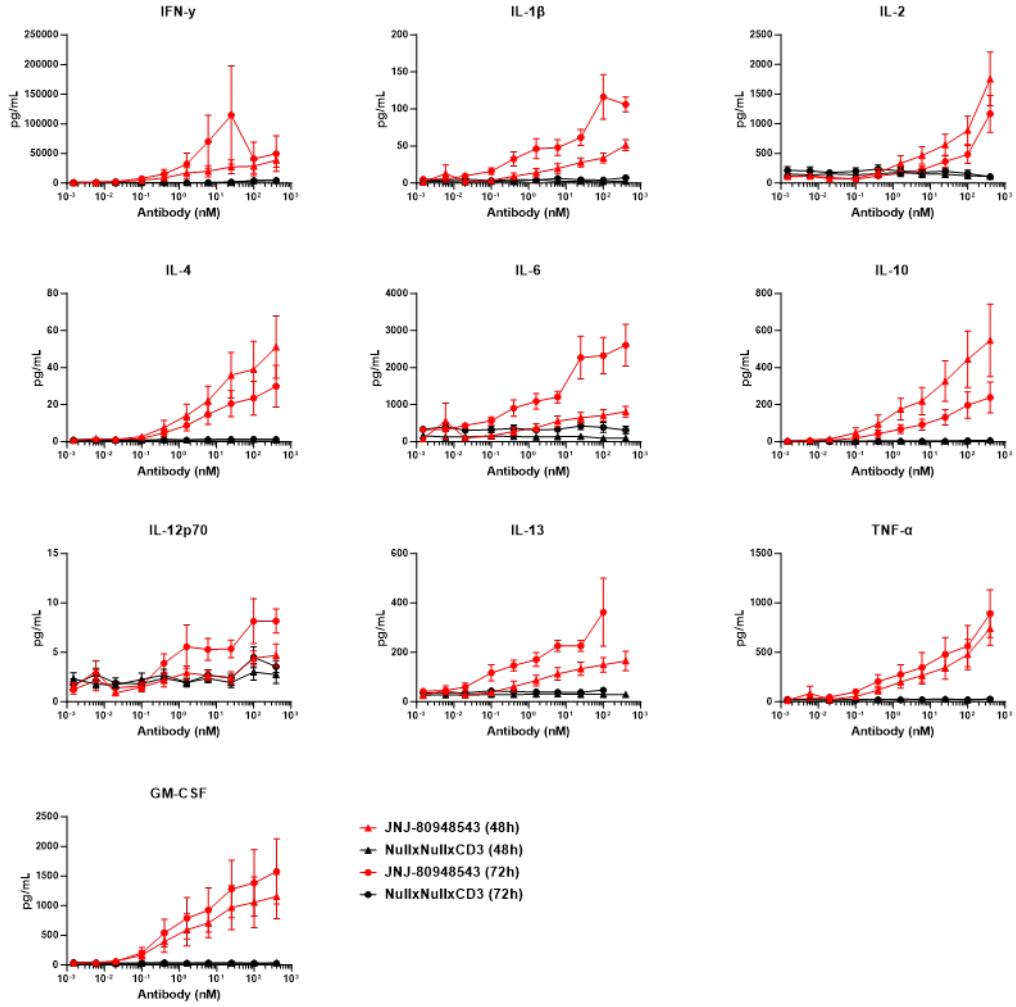

B.

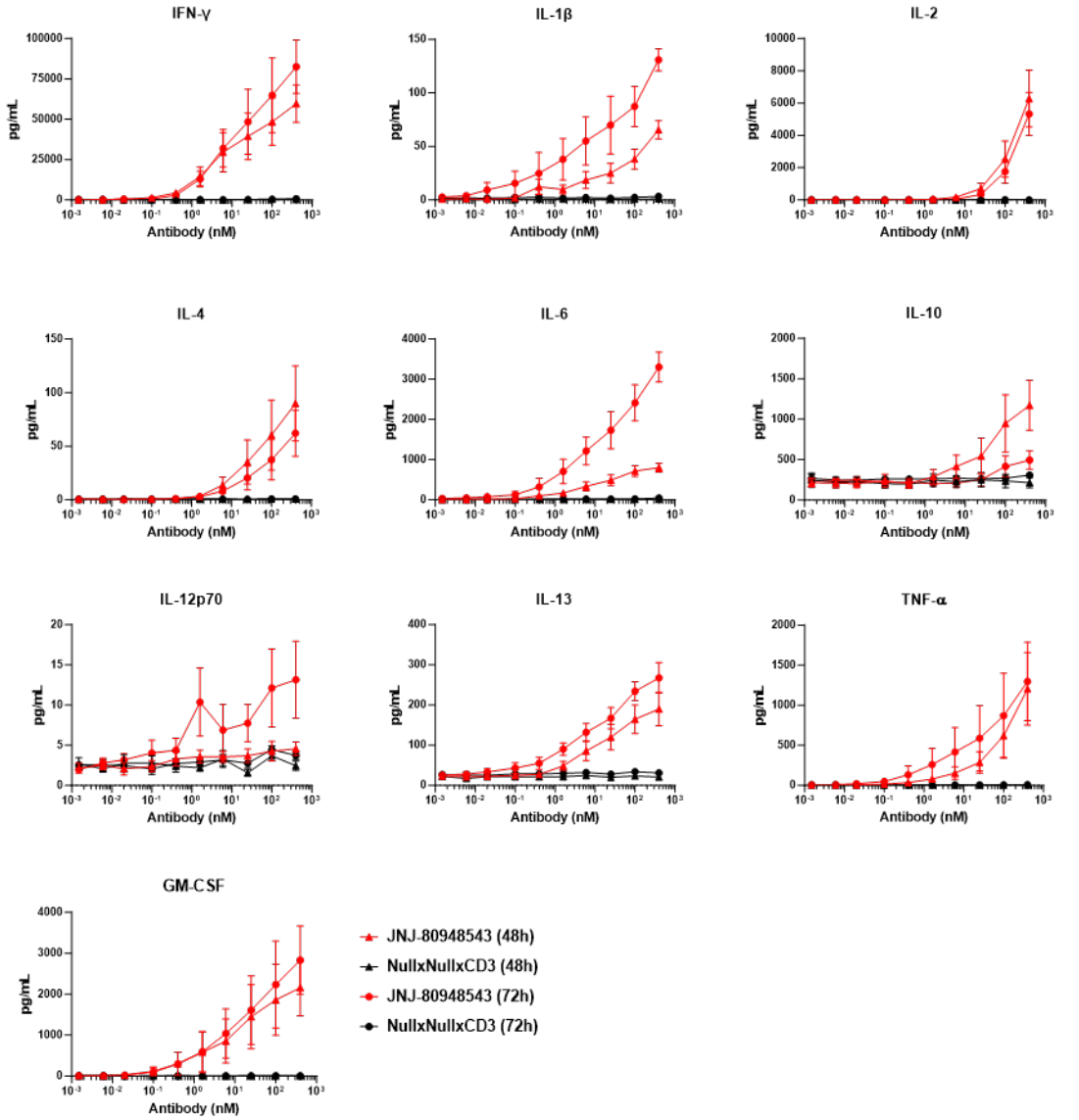
IFN-γ
IL-1β
IL-2
IL-4
IL-6
IL-10
IL-12p70
IL-13
TNF-α
GM-CSF
pg/mL
Antibody (nM)
JNJ-80948543 (48h)
NullxNullxCD3 (48h)
JNJ-80948543 (72h)
NullxNullxCD3 (72h)

C.

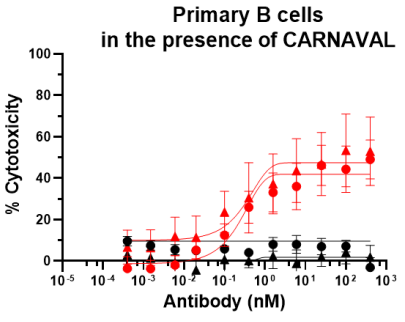
Primary B cells
in the presence of CARNAVAL
% Cytotoxicity
Antibody (nM)

D.

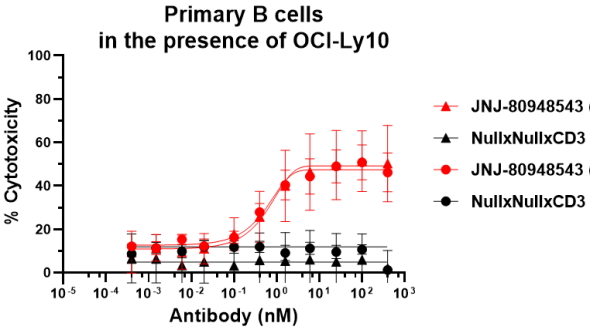
Primary B cells
in the presence of OCI-Ly10
% Cytotoxicity
Antibody (nM)
JNJ-80948543
NullxNullxCD3
JNJ-80948543
NullxNullxCD3

E.

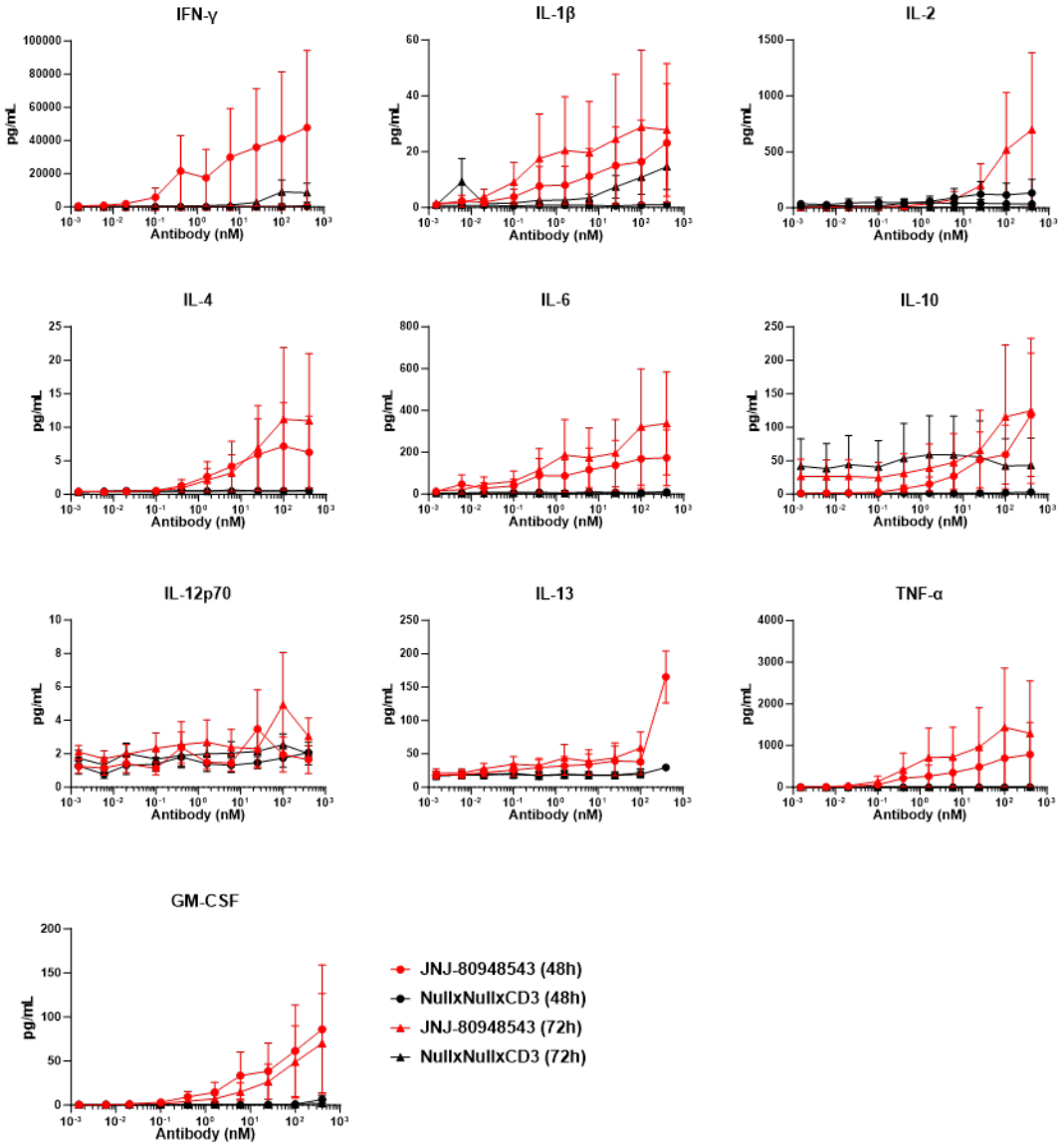

(A) Whole blood from 6 healthy donors was tested in T-cell redirection assays with the indicated antibodies and CD79b^{+}CD20^{+} CARNAVAL tumor cells. Cytokine levels were determined after 48 or 72 hours. The assay was conducted at an E:T ratio of 1:1; data were averaged and means ± SEM are graphed.

(B) Whole blood from 6 healthy donors was tested in T-cell redirection assays with the indicated antibodies and CD79b^{+}CD20^{+} OCI-Ly10 tumor cells. Cytokine levels were determined after 48 or 72 hours. The assay was conducted at an E:T ratio of 1:1; data were averaged and means ± SEM are graphed.

(C) and (D) Whole blood from 6 healthy donors was tested in whole-blood T-cell redirection assays with the indicated antibodies and CD79b^{+}CD20^{+} tumor cell lines, (C) CARNAVAL or (D) OCI-Ly10. The assay was conducted at an E:T ratio of 1:1 with respect to spiked-in tumor cells, but the E:T ratio for primary B cells ranged from 5:1 to 10:1. The percent cytotoxicity of primary B cells was determined after 48 or 72 hours. Data were averaged and means ± SEM are graphed.

(E) Whole blood from 6 healthy donors was incubated with the indicated antibodies (single point per condition per donor) for 48 or 72 hours. Cytokine production was measured; means ± SEM are graphed.

Supplemental Figure 7. Effect of JNJ-80948543 and JNJ-80948556 on OCI-Ly10 Tumor Volumes in T cell-humanized Mice

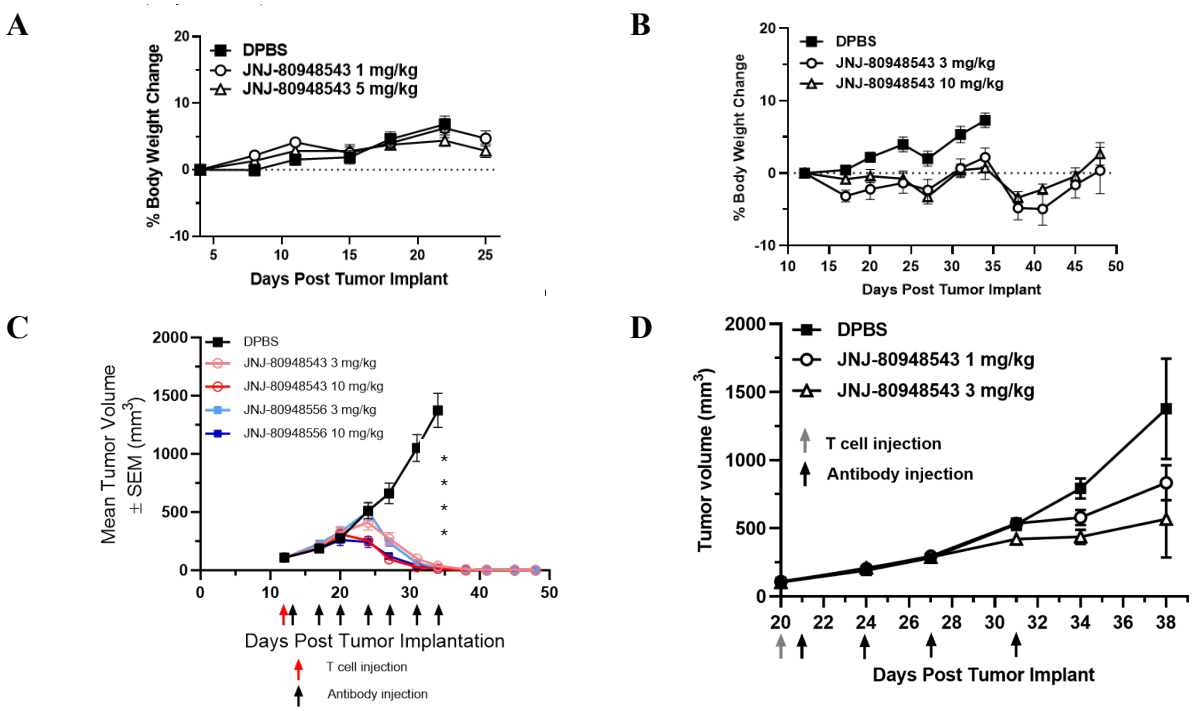

(A) Effect of JNJ 80948543 on Body Weight of T cell-humanized Mice Bearing SC CARNAVAL Tumors. Group body weights are graphed as the mean ± SEM (n=10/group). Tumor cells were implanted on Day 0, T cells were injected on Day 1, and mice were treated on Days 2, 5, 8, 11, 15, 18, 22, and 25. Data are displayed while at least 2/3 of animals remained in a group.

(B) Effect of JNJ-80948543 on Body Weight of T-cell-humanized Mice Bearing Established SC OCI-Ly10 Tumors. Group body weights are graphed as mean ± SEM (n=10/group). Tumor cells were implanted on Day 0, T cells were injected on Day 13, and dosing occurred on Days 14, 17, 20, 24, 27, 31, and 34. Data are displayed while at least 2/3 of animals remained in a group.

(C) T cell-humanized NSG mice injected SC with OCI-Ly10 tumors were dosed IP with JN48543 or JNJ-80948556 at 3 and 10 mg/kg for OCI-Ly10 (dosing time frame is denoted by bar below the X axis). Tumor volume was measured twice weekly and results presented as the mean tumor volume ± SEM for each group (n=10/group). Data are displayed while at least 2/3 of animals remained in a group. * Denotes significant difference ($p \leq 0.05$) compared with the DPBS control evaluated using a mixed model for repeated measures.

(D) OCI-Ly10 tumor cells were implanted on Day 0, T cells were injected on Day 20 when tumors reached a mean of 106 mm^3 (gray arrow), and dosing occurred on Days 21, 24, 27, and 31 (black arrows). Samples were collected for analysis 4, 24, 72, 96, and 168 hours post fourth dose. Tumor volumes are graphed as the mean ± SEM (n=15/group through Day 31; n=9/group on Day 34; n=3/group on Day 38).

Supplemental Methods

Null antibody generation

A null antibody for both the CD79b and CD20 arms (NullxNullxCD3) was generated as a negative control. In selected experiments, a NullxCD20xCD3 antibody was also generated and used. The fragment crystallizable (Fc) region of all the null antibodies was silent, as it contained the AAS mutations.

Cell lines

Human cell lines (CARNAVAL, JeKo-1, HT, SU-DHL-1, WILL-2, K562) were obtained from the American Type Culture Collection and Deutsche Sammlung von Mikroorganismen und Zellkulturen, or were licensed from the University of Toronto (OCI-Ly10). All cell lines were cultured at 37°C, 5% CO2 in complete culture medium (RPMI 1640 + GlutaMAX, 10% HI FBS) and tested negative for mycoplasma.

Parental CARNAVAL and OCI-Ly10 cells were transduced with Incucyte® NucLight Red lentiviral particles for expression of mKate2 red fluorescent protein. Flow cytometry-based sorting was performed to enrich the mKate2+ population, after which the pooled cells were kept under antibiotic selection.

Parental K562 cells were transduced with lentiviral particles containing a bicistronic plasmid encoding human CD79b-enhanced green fluorescent protein (eGFP) or CD20-mKate2. Antibiotic selection, with subsequent flow cytometry-based sorting, was performed to enrich CD79b+eGFP+ or CD20+mKate2+ expressing cells. To generate K562 cells expressing both CD79b-eGFP and CD20-mKate2, K562 CD79b-eGFP cells were transduced with lentiviral particles encoding CD20-mKate2. Flow cytometry-based sorting was performed to select for double-target-expressing cells, after which the cells were kept under antibiotic selection.

Pan T cells were collected from healthy donor leukopaks and isolated by negative selection. Frozen vials were stored in liquid nitrogen until use, then thawed and cells were transferred to fresh complete culture medium. Whole blood from healthy donors was collected in heparin tubes on the morning of the assay and stored at room temperature (RT) until plated.

Immunohistochemistry

To confirm specificity, the CD79 IHC antibody (clone D7V2F) was diluted at 1:100 and assessed by detection and absence of staining in $CD79b^+$ and $CD70^-$ cell lines. Tonsil tissue sections were included as positive controls for tissue staining of CD79b and CD20. The CD20 IHC antibody (clone L26) was ready-to-use purchased, validated by the vendor, and optimally diluted for use on the BOND system.

IHC staining, deparaffinization, and antigen retrieval process was performed on BOND RX automated stainer (Leica) using the BOND™ Polymer Refine Detection Kit. Epitope retrieval for CD79b was performed using BOND Epitope Retrieval Solution 2 at 100°C for 20 minutes, followed by 4 wash steps. For CD20, epitope retrieval was performed using BOND Epitope Retrieval Solution 1 at 100°C for 20 minutes, followed by 4 wash steps. Formalin-fixed paraffin-embedded (FFPE) tissues and tissue microarrays (TMA) were treated with 3% to 4% H_2O_2 for 5 minutes at RT to quench endogenous peroxidase activity, followed by a wash step (3 times with wash buffer). Anti-CD79b antibody and rabbit IgG (clone DA1E) isotype control were applied to the samples at 150 µL (0.15 µg/mL) per tissue and incubated for 30 minutes at RT. Anti-CD20 antibody was applied undiluted to the samples and incubated for 15 minutes at RT. After primary antibody incubation, tissues were washed 3 times with wash buffer, followed by adding a post-primary reagent rabbit anti-mouse IgG linker (to localize mouse antibodies) for 8 minutes at RT. The tissues were then treated with polymer anti-rabbit poly horseradish peroxidase – IgG for 10 minutes at RT, followed by 2 washes at 2 minutes each, and rinsed twice with distilled water. The refine reagent

3,3'-diaminobenzidine tetrahydrochloride hydrate was applied to tissues for 10 minutes at RT to visualize protein expression. Hematoxylin counterstain was applied and incubated for 5 minutes, followed by slide dehydration in a series of alcohols and xylene, then coverslipped.

All stained slides and TMAs were reviewed and scored by a Johnson & Johnson pathologist. All samples from relapsed/refractory lymphoma patients were scored based on percentage positive per neoplasm using staining intensity utilizing scores (0, 1+, 2+, or 3+). TMA was scored similarly. Scores were used for data representation.

Flow cytometry analysis of CD79b and CD20 expression on hematologic cancer cell lines

Quantum Simply Cellular microspheres were used according to manufacturer's instructions to correlate geometric mean fluorescence intensity with CD79b or CD20 antigen expression as molecules per cell on target positive and target negative cell lines. Values of isotype-stained cells were subtracted from values of cells stained for CD79b or CD20 to calculate receptor densities. Cells were considered negative for expression if the value was less than 2× the value of the isotype control.

CyTOF analysis of CD79b and CD20 expression on patient samples

Dissociated lymph node tissues from treatment-naïve B-NHL patients and patients with lymphadenitis (Fidelis or DLS) were stained with Rhodium-103 (Standard BioTools), followed by blocking of Fc receptors using human TruStain FcX (Biolegend). Cells were then stained with a Maxpar® Direct Immune Profiling Assay cocktail (MDIPA, Standard BioTools) supplemented with CD79b (clone CB3-1) and CD22 (clone HIB22). The cells were fixed in 1.6% formaldehyde solution and stained with Iridium-DNA intercalator (Standard Biotools). Prior to the acquisition, samples were resuspended in Maxpar® cell acquisition solution (Standard Biotools) containing 0.1x EQ™ four element calibration beads (Standard Biotools). Samples were acquired on the Helios mass cytometer (Standard BioTools).

Acquired FCS files were normalized using the processing module within the CyTOF® Software. All downstream gating and analyses were performed using the Cytobank software (Beckman Coulter).

CD79b and CD20 mRNA in silico analysis

Expressions of CD79b and CD20 (MS4A1) mRNA were extracted from extracted from an internal dataset from samples obtained from patients with different heme malignancies were profiled using the Affymetrix Human Genome U133 Plus2.0 microarray. These included 226 tissues samples which included acute myeloid leukemia (AML; n=39), CML (n=23), DLBCL (n=53), FL (n=76), MCL (n=14), multiple myeloma (MM) (n=19), myelodysplastic syndrome (MDS; n=1), monoclonal gammopathy of undetermined significance (MGUS; n=1), and non-malignant non-lymphoid tissue control samples collected from patients (n=9; DLBCL [n=4], FL [n=3], MCL [n=2]). The microarray probe sets were reannotated using the University of Michigan Brain Array custom CDF files (v20.0.0 – EntrezGene) and all samples were normalized in R 3.6.1 using the Robust Multi Average (RMA) normalization step present in the `affy` package (Bioconductor v3.2.0).

Off-Target Screening and Functional Specificity

The individual CD79b, CD20 and CD3 molecules were screened for binding specificity using the Retrogenix® Cell Microarray Technology screen (Charles River Laboratories). Briefly, test antibodies are screened against a library of 5,475 full-length human plasma membrane and cell-surface-tethered human secreted proteins and 371 heterodimers individually expressed on fixed HEK293 cells and detected with a AF647 anti-human secondary antibody. Specific interactions of the antigen binding domains are distinguished from antibody Fc or secondary antibody protein interactions.

For the functional specificity in vitro assay, tumor cell lines were selected from the Cancer Cell Line Encyclopedia (CCLE) transcriptomics data set. A panel of 6 cell lines were identified to be negative for CD79b, CD20 and CD3 (HEK-293T, K562, HCC-1833, HepG2, U87MG and SHP-77) that cumulatively express >50% of the known cell surface receptors using a cutoff of >5 TPM. Tumor cells and primary human T cells were plated at a 2:1 effector to target ratio and incubated with a titration of JNJ-80948543 or a NullxNullxCD3 control antibody. Supernatants were harvested 72 hours post treatment and assessed for cytokines (Granzyme B, IFNγ, IL-2 and TNFα) as a measure of antibody-induced T cell activation.

Incucyte® T-cell redirection assay using pan T cells and tumor targets

Tumor cell lines (CARNAVAL_mKate2, OCI-Ly10_mKate2, K562_CD79b_eGFP, K562_CD20_mKate2, K562_CD79b_eGFP_CD20_mKate2) were resuspended at 1×10^6 cells/mL in phenol-red-free complete medium.

JNJ-80948543 and NullxNullxCD3 antibodies were made at a 4× concentration of 400 nM in phenol-red-free complete medium and added to a 96-well U-bottom plate. The final antibody concentrations ranged from 100 nM to 0.1 pM.

Purified frozen pan T cells from 2 healthy donors were resuspended at 1×10^6 cells/mL in phenol-red-free complete medium. Pan T cells and tumor cells were combined at 1:1 and 5:1 effector-to-target (E:T) cell ratios and added to the serially diluted antibodies. Anti-CD25-Alexa 488 (1:1,000 dilution) was added to T cells cocultured with CARNAVAL_mKate2 or OCI-Ly10_mKate2 cells to measure T-cell activation over time. Analysis was performed on the Incucyte ZOOM live-content imaging system (Sartorius).

Images were automatically acquired in both phase and fluorescence channels every 6 hours for up to 6 days with a 4× objective lens (single image). Incucyte Zoom software (version

Incucyte 2019B Rev2) was used to detect target cells and T-cell activation based on mKate2 and CD25 expression, respectively, using optimized process definition parameters. For the analysis, the total red and green areas were quantified. For assessment of CD25 level, because CD25 signal in the first 48 hours showed high background fluorescence and provided a false positive signal, the scan values from the first 48 hours were excluded in further area under the curve (AUC) analysis. Beyond 48 hours, the background signal was sufficiently bleached and did not interfere with the readout. Data from different donors were graphed and AUC values were derived for each condition. After normalizing the data to the untreated control, antibody concentrations were plotted against the normalized values expressed as percent cytotoxicity as a concentration response

T-cell redirection assay using Pan T cells and tumor targets

CARNAVAL, OCI-Ly10, HT, WILL-2, JeKo-1, SU-DHL-1, and K562 cell lines were resuspended at 1×10^6 cells/mL in DPBS containing 0.1% bovine serum albumin (BSA) before incubation with carboxyfluorescein succinimidyl ester (CFSE; resuspended in 18 µL dimethyl sulfoxide and diluted 1:5,000) for 10 minutes at 37°C. Staining was quenched with 25 mL of complete medium, and cells were washed and resuspensed at 1×10^6 viable cells/mL in complete medium. JNJ-80948543 and NullxNullxCD3 antibodies were added to each well. For non-treated conditions, complete medium was added to the wells.

Purified frozen human pan T cells from 5 to 7 healthy donors were resuspended in complete medium at 3×10^6 cells/mL. Pan T cells and tumor cells were combined at 5:1 (all cell lines) and 1:1 (JeKo-1, CARNAVAL, OCI-Ly10) E:T ratios for each cell line, and the cell mixture was dispensed to the 96-well U-bottom plate containing the serially diluted antibodies. Plates were incubated at 37°C, 5% CO2 for 48 and 72 hours.

Supernatants were harvested for cytokine analysis. Cells were harvested to evaluate viability of tumor cells and T-cell activation. After cells were washed once in DPBS, viability was assessed by incubating the cells in Fixable Viability Dye eFluor™ 780 (diluted 1:1,000 in DPBS) for 30 minutes at 4°C. Viability staining was quenched by the addition of 100 µL/well of stain buffer, followed by centrifugation at 400× gravity (g) at RT for 5 minutes. Cells were resuspended in stain cocktail, incubated for 30 minutes at 4°C, and washed twice with 200 µL of stain buffer. Cell pellets were then resuspended in 100 µL of stain buffer and sample acquisition was performed on a FACSLyric flow cytometer (BD Biosciences). To assess cytotoxicity, the absolute count of the $CFSE^+$ cells was used to determine the number of viable cancer cells in each well. Viability of $CFSE^+$ cells was determined by using staining positivity of Fixable Viable cells in these assays were determined using Fixable Viability Dye eFluor™ 780.

The percentage of cytotoxicity was calculated using the formula:

$$\left(\frac{\text{Absolute \# of viable cancer cells}}{\text{Average of absolute \# of viable cancer cells in the untreated wells}}\right) \times 100$$

To measure the level of T-cell activation, the absolute percentage of CD69 and CD25 expression for either $CD4^+$ or $CD8^+$ T cells was used. It should be noted that SU-DHL-1 cells secrete IL-2 and IL-6 which will induce CD25 on T cells in the coculture system in the absence of antibodies. For the SU-DHL-1 coculture experiments only, the level of T-cell activation in the presence of antibodies was determined relative to the level of T-cell activation in the absence of antibodies.

Whole blood T-cell redirection assay

Fresh whole blood (50 µL) was added to Trucount tubes with 20 µL of BD Multitest staining mix. After incubation, the blood was lysed and fixed by adding 450 µL of 1× BD lysing solution. Lysed blood was acquired on a FACSLyric flow cytometer and the exact number of

T and B cells per µL of whole blood was calculated following the manufacturer's instructions for Trucount tube system.

JNJ-80948543 and NullxNullxCD3 were prepared at 4× concentration (1600 nM) and serially diluted at concentrations ranging from 400 nM to 0.38 pM for assay use. Two types of assays were performed, either with or without spiked-in, labeled cancer cells. In the spiked-in cancer cell setting, CARNAVAL and OCI-Ly10 cells cultured in complete medium were washed with DPBS containing 0.1% BSA and CFSE dye, and reconstituted and added to the cells as previously described, followed by incubation for 10 minutes at 37°C. Cold complete medium was added to quench the labeling and the cells were centrifuged at 400×g at RT for 4 minutes, washed, and counted. An E:T ratio of 1:1, with T cells from whole blood as effectors, and target cells comprising spiked-in labeled CARNAVAL or OCI-Ly10 tumor cells and primary B cells in the donor blood, were used. CFSE-labeled target cells were diluted in complete medium to the specific density required to achieve a 1:1 E:T ratio when adding 50 µL of the cell suspension per well to 100 µL of whole blood. In a 96-well U-bottom plate, 50 µL of the CFSE-labeled target cells were dispensed first for the spiked-in assay, while in the autologous assay, no CFSE-labeled target cells were added, but 50 µL of complete medium was added. Next, 50 µL of the 4× concentrated antibody dilution series were added to the wells, followed by 100 µL of whole blood. For each donor, single wells were tested per condition. Plates were incubated at 37°C, 5% CO2 for 48 or 72 hours.

After each timepoint, cells were harvested to evaluate viability of tumor cells and T-cell activation. Plates were centrifuged at 400×g for 3 minutes. From each well, serum supernatant was harvested for cytokine analysis. Blood and cell pellets were lysed with 200 µL/well of RBC lysis buffer, incubated at RT for 5 minutes, and centrifuged for 5 minutes at 400×g. The lysis process was repeated 4 more times, and cells were washed once in DPBS and resuspended in 100 µL of 1:1,000 diluted Fixable Viability Dye eFluor™ 780 in DPBS,

followed by incubation for 30 minutes at 4°C in the dark. Cells were centrifuged for 5 minutes at 400×g and after removing the supernatant, resuspended in 100 µL/well of Fc blocking reagent and incubated for 10 minutes at RT in the dark. Cells were then centrifuged for 5 minutes at 400×g and pellets were resuspended in 100 µL staining cocktail and incubated for 30 minutes in the dark at 4°C. Cells were acquired on a LSRFortessa flow cytometer (BD Biosciences).

Tumor cells or primary B cells were identified by gating on FSC and SSC to identify cell populations followed by $CFSE^{+}$ (tumor cells) or CFSE- followed by staining for $CD19^{+}$(primary B cells). LIVE/DEAD staining was performed to evaluate cell death.

T-cell activation were identified by gating on FSC and SSC to identify cell populations, then $CFSE^{-}$ to identify the blood population, followed by $CD3^{+}$ to identify T cells. LIVE/$DEAD^{-}$ staining was performed for live T cells. $CD4^{+}$ and $CD8^{+}$ subsets were identified and from each subset, CD69 and CD25 expression was determined.

Cytokine assay

Supernatants from the flow-cytometry based T-cell redirection assays were tested using the Human Pro-inflammatory Panel 1 kit (MSD). Frozen supernatants were diluted 1:10 in Diluent 2. A standard curve was prepared by reconstituting and serially diluting the provided calibrator in Diluent 2 as per the manufacturer's protocol. MSD Assay Plates (V Plex Proinflammation Panel 1 [human] kit) were prewashed per manufacturer's protocol and filled with the diluted supernatant or standards as per plate layout. Plates were incubated for 2 hours at RT followed by 2 hours of incubation with the antibody solution. Assay plates were read on a SECTOR imager (MSD). For serum cytokine samples from the whole-blood assays, an additional single-plex analysis from MSD for granulocyte-macrophage colony-stimulating factor (GM-CSF) was also performed according to the manufacturer's protocol. Extrapolation

of sample values from the standard curve for each cytokine was performed using the DISCOVERY WORKBENCH software (MSD, Version 4.0).

Antagonistic activity assay

OCI-Ly10 cells were harvested and resuspended at 9.52×10^5 cells/mL and added to U-bottom 96-well plate.

JNJ-80948543, CD79bxNullxCD3, NullxCD20xCD3, and NullxNullxCD3 antibodies were prepared at a 4× concentration of 4 μM in complete medium. A total of nine 3-fold serial dilutions were made and 35 μL of diluted antibody were added to each well of the 96-well plate. The final antibody concentrations tested in the assay ranged from 1 μM to 0.03 nM. As a control, complete culture medium containing 2.7% DPBS was prepared and added to the appropriate wells. The plates were incubated at 37°C, 5% CO2 for 24 hours.

After incubation, the plates were centrifuged at 800 rpm for 5 minutes and 50 μL of supernatant were transferred to a prewashed MSD Assay Plate (V Plex Proinflammation Panel 1 [human] kit). The MSD assay was performed as described per manufacturer's protocol, and the plates were read on a SECTOR imager (MSD). Cell viability was assessed in parallel after 24 hours incubation using CellTiter-Glo® Luminescent Cell Viability Assay glow according to the manufacturer's recommendations.

Xenograft mouse models

For all studies, female NSG mice (Charles River Laboratories) approximately 7 to 14 weeks of age and weighing approximately 25 g were used. All experiments were carried out in accordance with *The Guide for the Care and Use of Laboratory Animals* and were approved by the Institutional Animal Care and Use Committee of Johnson & Johnson, Beerse, Belgium.

CARNAVAL and OCI-Ly10 cells were cultured and harvested in their respective complete culture medium. On the day of tumor implantation, CARNAVAL cells were resuspended in

cold (4°C) serum-free medium at 5×10^6 cells/mL. OCI-Ly10 cells were resuspended in cold serum-free medium + Matrigel® (diluted 1:1) at 5×10^6 cells/mL.

Human pan-T cells were activated and expanded in vitro using the T-cell activation and expansion kit and grown in T-cell complete culture medium containing interleukin (IL)-2 at a concentration of 10 ng/mL, starting 3 days after thaw and activation. On the day of engraftment into mice, activation beads were removed from the T cells and cells were resuspended in serum-free medium at a concentration of 1×10^8 cells/mL, for an IP injection of 2×10^7 cells in 0.2 mL per mouse.

In all studies, T-cell-humanized mice were given fragment crystallizable (Fc) block at 0.2 mg/mouse IP and human immune globulin infusion at 10 mg/mouse IP at least 30 minutes prior to antibody dosing, to compensate for the low immunoglobulin environment in the NSG mouse strain.

In the prevention efficacy study, mice were randomized into groups of 10 and injected SC in the right flank with 1×10^6 CARNAVAL cells (0.2 mL). On Day 1, mice were humanized with T cells and starting on Day 2, mice were treated twice a week IP with 25 or 125 µg JNJ-80948543 (corresponding to 1 or 5 mg/kg, respectively) or DPBS, for a total of 8 doses.

In the established efficacy study, mice were injected SC in the right flank with 1×10^6 OCI-Ly10 cells (0.2 mL). On Day 12, mice were randomized into groups of 10 by tumor volume (mean tumor volume of 108 mm^3) and humanized with T cells on Day 13. On Day 14, mice were treated twice a week with IP dosing of 75 or 250 µg JNJ-80948543 or JNJ-80948556 (corresponding to 3 or 10 mg/kg, respectively) or DPBS, for a total of 7 doses.

To assess PD of JNJ-80948543 in established OCI-Ly10 tumors. Mice were injected SC in the right flank with 1×10^6 OCI-Ly10 cells in 0.2 mL. On Day 20, mice were randomized into groups of 15 by tumor volume (mean tumor volume of 106 mm3) and humanized with T

cells. On Day 21, treatment was initiated with IP dosing twice a week for a total of 4 doses of 25 or 75 µg of JNJ-80948543 (corresponding to 1 or 3 mg/kg, respectively) or DPBS. Tumors were collected from 3 animals per group and timepoint at 4, 24, 72, 96, and 168 hours post fourth dose to evaluate T cell infiltration by immunohistochemistry (IHC) analysis.

Tumor volume in SC models was calculated using the formula: tumor volume (mm^3) = ($D \times d^2/2$); where 'D' represents the larger diameter, and 'd' the smaller diameter of the tumor as determined by caliper measurements.

The percent TGI was defined as the difference between mean tumor volumes of the treated and control groups, calculated as % TGI = $((TV_c-TV_t)/TV_c)\times100$ where 'TV_c' is the mean tumor volume of the control group and 'TV_t' is the mean tumor volume of the treatment group. As defined by National Cancer Institute (NCI) criteria, ≥60% TGI is considered biologically significant.

The percent ΔTGI was defined as the difference between mean tumor volume of the treatment and control groups, calculated as % ΔTGI = $([(TV_c-TVc_0)-(TV_t-TVt_0)]/(TV_c-TV_{c0}))\times100$ where 'TV_c' is the mean tumor volume of a given control group, 'TV_{c0}' is the mean initial tumor volume of a given control group, 'TV_t' is the mean tumor volume of the treatment group, and 'TV_{t0}' is the mean initial tumor volume of the treatment group.

A CR for SC tumor models was defined as complete tumor regression, with no palpable tumor on the day of analysis.

Tumor volume was graphed using Prism. Statistical significance for most studies was evaluated for antibody-treated groups compared with controls on the last day of the study when at least two thirds of the control animals were still on study.

Animal Monitoring

Body weight and SC tumor volume were measured at least twice a week throughout each study. Animals were monitored daily for clinical signs related to graft versus host disease (GvHD; caused by human immune cells reacting to mouse tissue antigens) or tumor burden. When individual animals exhibited negative clinical signs, such as lethargy, ruffled and matted coat, hunched posture, cyanotic extremities, or dyspnea, or reached 20% body weight loss as compared with initial body weights, they were removed from the study and humanely euthanized. In the absence of negative clinical signs, animals were removed from SC tumor studies when a maximum tumor volume of $\geq$1,400 mm^3 was reached.